การสังเคราะห์ท่อนาโนไทเทเนตและการประยุกต์ใช้เป็นตัวรองรับตัวเร่งปฏิกิริยาแพลเลเดียม

นาย สมจิตร พุฒดี

วิทยานิพนธ์นี้เป็นส่วนหนึ่งของการศึกษาตามหลักสูตรปริญญาวิศวกรรมศาสตรมหาบัณฑิต
สาขาวิชาวิศวกรรมเคมี ภาควิชาวิศวกรรมเคมี
คณะวิศวกรรมศาสตร์ จุฬาลงกรณ์มหาวิทยาลัย
ปีการศึกษา 2553

SYNTHESIS OF TITANATE NANOTUBES AND THEIR APPLICATIONS AS Pd CATALYST SUPPORT

Mr. Somjit Putdee

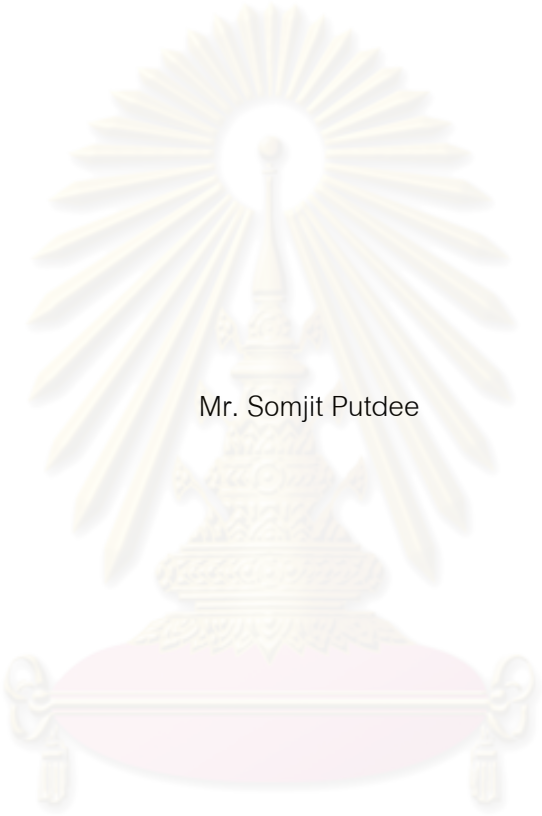

A Thesis Submitted in Partial Fulfillment of the Requirements
for the Degree of Master of Engineering Program in Chemical Engineering

Department of Chemical Engineering
Faculty of Engineering
Chulalongkorn University

Academic Year 2010

Thesis Title	SYNTHESIS OF TITANATE NANOTUBES AND THEIR APPLICATIONS AS Pd CATALYST SUPPORT
By	Mr. Somjit Putdee
Field of Study	Chemical Engineering
Thesis Advisor	Assistant Professor Joongjai Panpranot, Ph.D.
Thesis Co-advisor	Apinan Soottitantawat, Ph.D.

Accepted by the Faculty of Engineering, Chulalongkorn University in Partial Fulfillment of the Requirements for the Master's Degree

.....Dean of the Faculty of Engineering

(Associate Professor Boonsom Lerdhirunwong, Dr.Ing.)

THESIS COMMITTEE

A. Arpornwichanop
..... Chairman

(Assistant Professor Amornchai Arpornwichanop, D.Eng.)

..... Thesis Advisor

(Assistant Professor Joongjai Panpranot, Ph.D.)

..... Thesis Co-advisor

(Apinan Soottitantawat, Ph.D.)

..... Examiner

(Akawat Sirisuk, Ph.D.)

..... External Examiner

(Assistant Professor Okorn Makasuwandamrong, D.Eng.)

สมจิตร พุฒดี : การสังเคราะห์ท่อนาโนไทเทเนตและการประยุกต์ใช้เป็นตัวรองรับตัวเร่งปฏิกิริยาแพลเลเดียม. (SYNTHESIS OF TITANATE NANOTUBES AND THEIR APPLICATIONS AS Pd CATALYST SUPPORT) อ. ที่ปรึกษาวิทยานิพนธ์หลัก : ผศ.ดร. จูงใจ ปิ้นประณต, อ. ที่ปรึกษาวิทยานิพนธ์ร่วม : ดร.อภินันท์ สุทธิธารธวัช, 84 หน้า.

งานวิจัยนี้ได้ทำการสังเคราะห์ท่อนาโนไทเทเนตและเส้นนาโนไทเทเนตโดยวิธีไฮโดรเทอร์มอลจากไทเทเนียทรงกลมเชิงการค้า โดยศึกษาผลของการทำให้เย็นอย่างรวดเร็ว อุณหภูมิปฏิกิริยาและการเผา ต่อการเกิดและรูปร่างของไทเทเนต พบว่าท่อนาโนไทเทเนตที่มีพื้นที่ผิวสูงสังเคราะห์ได้ที่อุณหภูมิ 150 องศาเซลเซียส เมื่อเพิ่มอุณหภูมิปฏิกิริยาเป็น 200 องศาเซลเซียส ท่อนาโนไทเทเนตเปลี่ยนรูปร่างไปเป็นเส้นนาโนไทเทเนต การเผาที่ 600 องศาเซลเซียส ทำให้ท่อนาโนไทเทเนตเปลี่ยนรูปร่างกลับไปเป็นอะนาเทสไทเทเนีย ในขณะที่การเผาเส้นนาโนไทเทเนตเปลี่ยนเป็นไทเทเนียแบบเมตะสเตเบิลภายใต้สภาวะเดียวกัน การใช้ท่อนาโนไทเทเนตเป็นตัวรองรับตัวเร่งปฏิกิริยาแพลเลเดียม ส่งผลให้ประสิทธิภาพการเร่งปฏิกิริยาในปฏิกิริยาไฮโดรจิเนชันแบบเลือกเกิดของหนึ่ง-เฮปไทน์ในวัฏภาคของเหลวสูงกว่าตัวเร่งปฏิกิริยาแพลเลเดียมที่เตรียมบนเส้นนาโนไทเทเนตและไทเทเนียทางการค้า ตัวเร่งปฏิกิริยาแพลเลเดียมบนท่อนาโนไทเทเนตที่เตรียมจากวิธีรีดักชันด้วยตัวทำละลายแสดงค่าการเปลี่ยนของหนึ่ง-เฮปไทน์ที่สูงกว่าตัวเร่งปฏิกิริยาที่เตรียมโดยวิธีการเคลือบฝัง ในขณะที่อัตราการเกิดปฏิกิริยาไฮโดรจิเนชันเพิ่มขึ้นเมื่อการกระจายตัวของแพลเลเดียมสูงขึ้น ค่าการเลือกเกิดเป็นหนึ่ง-เฮปทีนขึ้นกับชนิดของตัวรองรับ และ/หรืออันตรกิริยาระหว่างแพลเลเดียมและตัวรองรับ

ภาควิชา วิศวกรรมเคมี ลายมือชื่อนิสิต สมจิตร พุฒดี

สาขาวิชา วิศวกรรมเคมี ลายมือชื่อ อ.ที่ปรึกษาวิทยานิพนธ์หลัก

ปีการศึกษา 2553 ลายมือชื่อ อ.ที่ปรึกษาวิทยานิพนธ์ร่วม

5270529821 : MAJOR CHEMICAL ENGINEERING

KEYWORDS : TITANIA / TITANATE NANOTUBES / HYDROTHERMAL / Pd NANOPARTICLES / 1-HEPTYNE HYDROGENATION

SOMJIT PUTDEE : SYNTHESIS OF TITANATE NANOTUBES AND THEIR APPLICATIONS AS Pd CATALYST SUPPORT. ADVISOR : ASST. PROF. JOONGJAI PANPRANOT, Ph.D., CO-ADVISOR : APINAN SOOTTITANTAWAT, Ph.D., 84 pp.

In this research, titanate nanotubes and nanowires were synthesized by hydrothermal method from a spherical shape commercial TiO_2. The effects of quenching, reaction temperature, and annealing on the formation and morphology of the titanate were investigated. Titanate nanotubes with high BET surface area were synthesized at 150 °C. The titanate nanotubes were transformed to titanate nanowires when the reaction temperature was increased to 200 °C. After annealing at 600 °C, the titanate nanotubes transformed back into anatase TiO_2 whereas annealing of the titanate nanowires resulted in metastable form TiO_2 under similar conditions. The use of titanate nanotubes as Pd catalyst support resulted in higher catalytic performance in the liquid phase selective hydrogenation of 1-heptyne than the Pd catalysts supported on titanate nanowire and commercial titania. The titanate nanotubes supported Pd nanoparticles synthesized from reduction by solvent method exhibited higher conversion of 1-heptyne than those prepared by impregnation method. While the hydrogenation rate increased with increasing Pd dispersion, the selectivity to 1-heptene depended largely on the nature of TiO_2 support and/or the interaction of Pd and titania support.

Department : Chemical Engineering	Student's Signature Somjit Putdee
Field of Study : Chemical Engineering	Advisor's Signature
Academic Year : 2010	Co-advisor's Signature

ACKNOWLEDGEMENTS

First of all, the author would like to express my sincere and deepest appreciation to my advisor and co-advisor, Assistant Professor Joongjai Panpranot and Dr. Apinan Soottitantawat for their invaluable suggestions, support, encouragement, and help during the course of my graduate study. Without the continuous guidance and comments from Professor Piyasan Praserthdam, this work would never have been achieved. In additional, the author would also be grateful to Assistant Professor Amornchai Arpornwichanop, as the chairman, Dr. Akawat Sirisuk, and Assistant Professor Okorn Makasuwandamrong as the members of the thesis committee.

Most of all, the author would like to express his highest gratitude to his parents who always pay attention to him all the times for their suggestions and have provided support and encouragements. The most success of graduation is devoted to his parents.

Moreover, the author wishes to thank the members of the Center of Excellence on Catalysis and Catalytic Reaction Engineering, Department of Chemical Engineering, Faculty of Engineering, Chulalongkorn University and the member of Chemical Engineering Laboratory for their friendship and assistance. To the many others, not specifically named, who have provided his with support and encouragement, please be assured that he thinks of you.

Finally, the author would like to thank the Thailand Research Fund (TRF), as well as the Graduate School of Chulalongkorn University for their financial supports.

CONTENTS

CHAPTER Page

CHAPTER Page

CHAPTER Page

LIST OF TABLES

LIST OF FIGURES

FIGURE Page

CHAPTER I

INTRODUCTION

1.1 Rationale

Catalytic hydrogenation is one of the most useful, versatile, and environmentally acceptable reaction routes available for organic synthesis, because the scope of there action type is very broad and many functional groups can be hydrogenated with high selectivity and high conversation [1]. The selective alkyne hydrogenation is the important reaction for the preparation of fine chemicals and biologically activity compounds [1-4]. The main objective of alkyne semihydrogenation is to achieve the highest alkene selectivity. In these cases, avoiding over hydrogenation to single bonds is an important requirement.

Heterogeneous catalysts for carbon-carbon multiple bond hydrogenation contain noble metals such as Pd, Pt, Ru, and Rh, which are highly active and selective. Many researchers have found that supported palladium (Pd) catalysts present the highest catalytic activity for the semihydrogenation of alkynes to alkenes [2-5]. The notable advantages of supported noble metal catalysts under heterogeneous conditions are relatively high activity, mild process conditions, easy separation, and better handling properties [2]. Several supports have been employed for Pd catalysts in the selective alkyne hydrogenation including SiO_2 [1, 3], Al_2O_3 [5], and TiO_2 [4].

Titania and titanate nanotubes have attracted considerable attention for their potential applications in a variety of areas, such as solar cells, hydrogen storage, gas sensors, photocatalysis, and catalyst supports because of their high surface area, porosity, low cost, and chemical stability [6-8]. There are three main methods for preparation titanates nanotubes: the template method, anodic oxidation, and the hydrothermal method. Among these methods, hydrothermal method received wide investigations because of low cost, easy route to obtain nanotubes, and the feasibility of wide spread applications [9]. Applied reaction temperature, reaction time, concentration of NaOH, size of raw TiO_2 powder are considered as the predominant factors in the formation of nanotubes [10, 11]. However, the effects of quenching and

annealing treatments on the properties of titanates have not been reported to much of a degree.

Most researchers focus on the use of titanate nanotubes as photocalalysis, gas sensors, and solar cell. However, using titanate nanotubes as catalyst support have not been studied to much degree. In addition, there are no reports on the use of Pd catalysts supported on titanate nanotubes in the liquid-phase hydrogenation. In this study, liquid phase hydrogenation of 1-heptyne over Pd supported titania, titanate nanotubes, and nanowire was investigated.

1.2 Objectives

1. To investigate the effect of preparation conditions on the formation of titanate nanotubes and nanowires during hydrothermal synthesis.
2. To investigate the effect of quenching and annealing post treatment on the transformation and morphology of the synthesized titanate.
3. To investigate the characteristics and catalytic properties of Pd nanoparticles supported on titania, titanate nanotubes, and nanowires in the liquid-phase selective hydrogenation of 1-heptyne.
4. To compare the effect of different methods for preparation Pd nanoparticles by reduction by solvent and conventional wet impregnation method.

1.3 Research Scopes

Part I

- Synthesis titanate nanotubes and nanowires by hydrothermal method at various reaction temperatures between 110°C-200°C
- Study the effect of annealing and quenching on the transformation and morphology of titanate nanotubes and nanowire.

Part II

- Synthesis of palladium colloid nanoparticles using reduction by solvent method under an argon atmosphere.
- Preparation of titania and titanate supported palladium catalysts using Pd colloid nanoparticles and wet impregnation method with palladium loading of ca. 1 wt %.
- Characterization of the catalysts using several techniques, such as X-ray diffraction (XRD), N_2 physisorption, transmission electron microscopy (TEM), scanning electron microscopy (SEM), pulse CO chemisorption, X-ray photoelectron spectroscopy (XPS), and inductively coupled plasma (ICP)
- The catalytic performance of the titania and titanate supported palladium catalysts was studied in the liquid-phase selective hydrogenation of 1-heptyne to heptene using stirring batch reactor (stainless steel autoclave 50 ml).

1.4 Research Methodology

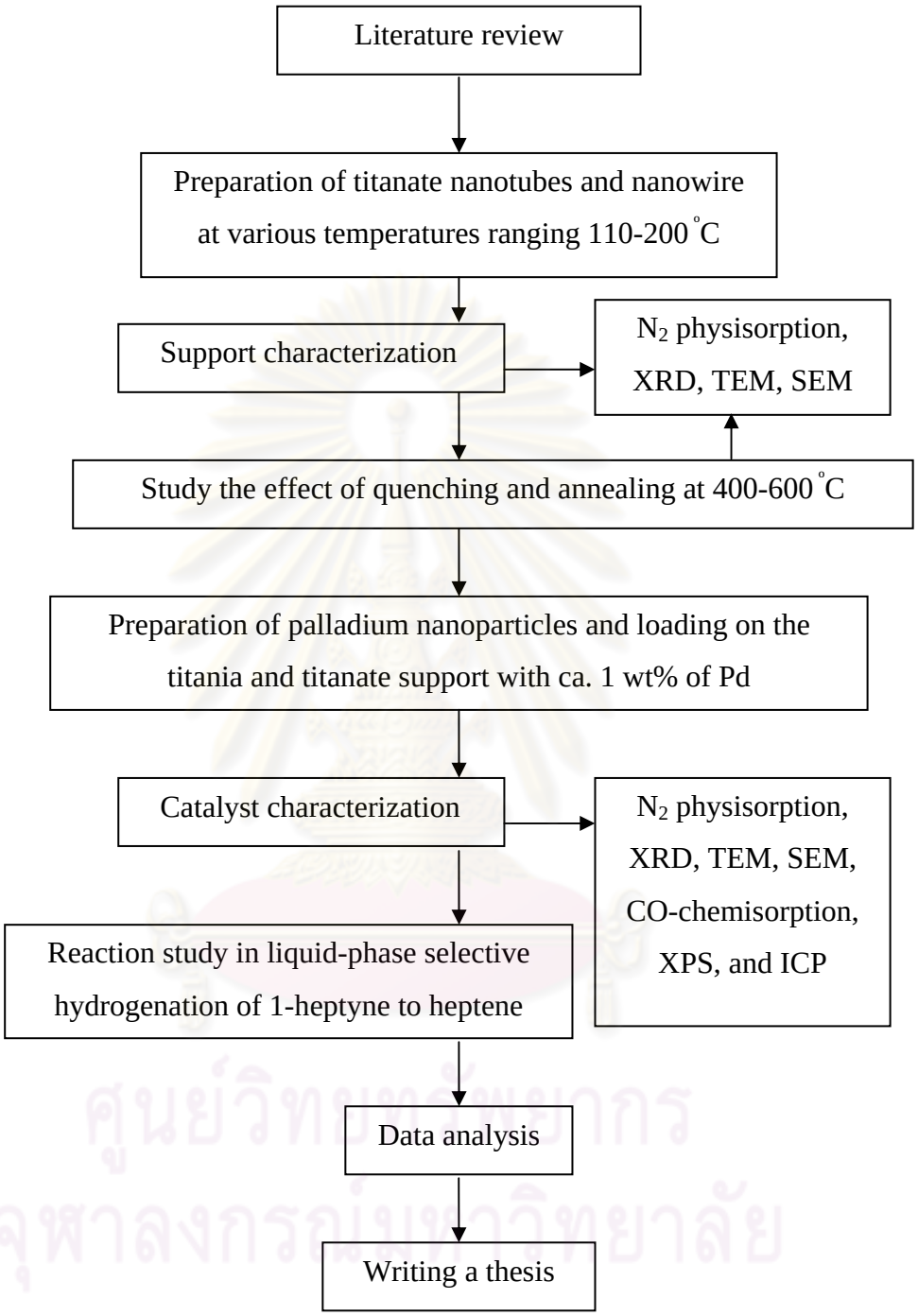

CHAPTER II

THEORY

2.1 Titanium dioxide

2.1.1 Physical and chemical properties

Titanium (IV) oxide occurs naturally in three crystalline forms:

1. Anatase, which tends to be more stable at low temperatures. Anatase TiO_2 generally exhibits a higher activity in hydrogenation and photocatalytic than other types of titanium dioxide. The three forms of titanium (IV) oxide have been prepared in laboratories but only rutile, the thermally stable form, has been obtained in the form of transparent large single crytal. The transformation from anatase to rutile is accompanied by the evolution of ca. 12.6 kJ/mol (3.01 kcal/mol), but the rate of transformation is greatly affected by temperature and the presence of other substances, which may either catalyze or inhibit the reaction. The lowest temperature at which transformation from anatase to rutile takes place at a measurable rate is around 700 ◦C, but this is not a transition temperature. The change is not reversible since ΔG for the change from anatase to rutile is always negative.

2. Brookite, which is usually found only in minerals and has a structure brlonging to orthorhombic crystal system. Brookite has been produced by heating amorphous titanium (IV) oxide, which is prepared from an alkyl titanate or sodium titanate, with sodium or potassium hydroxide in an autoclave at 200 to 600 ◦C for several days.

3. Rutile, which tends to be more stable at high temperature and thus is sometimes found in igneous rocks. The titanium dioxide use in industrial products, such as paint, is almost a rutile type. These crystals are substantially pure titanium dioxide but usually amount of impurities, e.g., boron, Magnesium or calcium, which darken them. The important commercial forms of titanium (IV) oxide are anatase and

rutile, and they can readily be distinguished by X-ray diffractometry. A summary of crystallographic properties of the three varieties is given in Table 2.1

Table 2.1 Crystallographic properties of anatase, brookite, and rutile

Properties	**Anatase**	**Brookite**	**Rutile**
Crystal structure	Tetragonal	Orthorhombic	Tetragonal
Optical	Uniaxial, Negative	Biaxial, positive	Uniaxial, Negative
Density, g/cm^3	3.9	4.0	4.23
Harness, Mohs scale	$5\frac{1}{2}$ - 6	$5\frac{1}{2}$ - 6	7 - $7\frac{1}{2}$
Unit cell	D_4a^{19} . $4TiO_2$	D_2h^{15} . $8TiO_2$	D_4h^{12} . $3TiO_2$
Dimension, nm			
a	0.3758	0.9166	0.4584
b		0.5436	
c	0.9514	0.5135	2.953

The three allotropic forms of titanium dioxide have been prepared artificially but only rutile, the thermally stable form, has been obtained in the form of transparent large single crystal. The transformation form anatase to rutile is accompanied by the evolution of ca. 12.6 kJ/mol (3.01 kcal/mol), but the rate of transformation is greatly affected by temperature and by the presence of other substance which may either catalyze of inhibit the reaction. The lowest temperature at which conversion of anatase to rutile takes place at a measurable rate is ca. 700°C, but this is not a transition temperature. The change is not reversible; ΔG for the change from anatase to rutile is always negative.

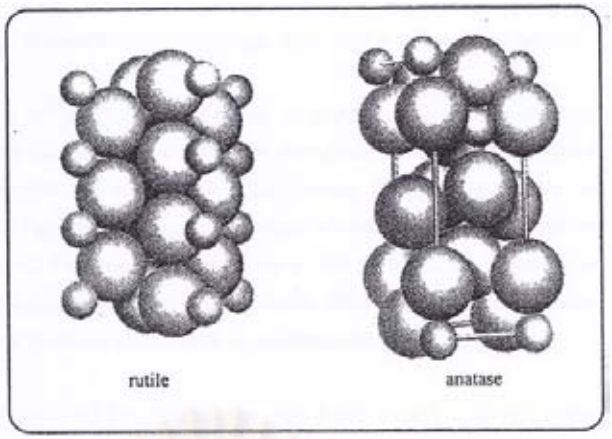

Figure 2.1 Crystal structures of titanium dioxide in rutile, and anatase

Although anatase and rutile are both tetragonal, they are not isomorphous (Figure 2.1). The two tetragonal crystal types are more common because they are easy to make. Anatase occurs usually in near-regular octahedral, and rutile forms slender prismatic crystal, which are frequently twinned. Rutile is the thermally stable form and is one of the two most important ores of titanium.

Since both anatase and rutile are tetragonal, they are both anisotropic, and their physical properties, e.g. refractive index, vary according to the direction relative to the crystal axes. In most applications of these substances, the distinction between crystallographic directions is lost because of the random orientation of large numbers of small particles, and it is mean value of the property that is significant.

Measurement of physical properties, in which the crystallographic directions are taken into account, may be made of both natural and synthetic rutile, natural anatase crystal, and natural brookite crystals. Measurement of the refractive index of titanium dioxide must be made by using a crystal that is suitably orientated with respect to the crystallographic axis an as a prism in a spectrometer. Crystals of suitable size of all three modifications occur naturally and have been studied. However, rutile is the only form that can be obtained in large artificial crystals form melts. The refractive index of rutile is 2.75. The dielectric constant of rutile varies with direction in the crystal and with any variation from the stoichiometric formula, TiO_2; an average value for rutile in powder form is 114. The dielectric constant of anatase powder is 48.

Titanium dioxide is thermally stable (mp 1855 °C) and very resistant to chemical attack. When it is heated strongly under vacuum, there is a slight loss of oxygen corresponding to a change in composition to $TiO_{1.97}$. The product is dark blue but reverts to the original white color when it is heated in air.

Hydrogen and carbon monoxide reduce it only partially at high temperatures, yielding lower oxides or mixtures of carbide and lower oxides. At ca. 2000°C and under vacuum, carbon reduces it to titanium carbide. Reduction by metal, e.g., Na, K, Ca, and Mg, is not complete. Chlorination is only possible if a reducing agent is present; the position of equilibrium in the system is the reactivity of titanium dioxide towards acid is very dependent on the temperature to which it has been heated. For example, titanium dioxide that has been prepared by precipitation from a titanium (IV) solution and gently heated to remove water is soluble in concentrated hydrochloric acid. If the titanium dioxide is heated to ca. 900 °C, then its solubility in acids is considerably reduced. It is slowly dissolve in hot concentrate sulfuric acid, the rate of salvation being increased by the addition of ammonium sulfate, which raises the boiling point of the acid. The only other acid in which it is soluble is hydrofluoric acid, which is used extensively in the analysis of titanium dioxide for trace elements. Aqueous alkaline have virtually no effect, but molten sodium and potassium hydroxides, carbonates, and borates dissolve titanium dioxide readily. An equimolar molten mixture of sodium carbonate and sodium borate is particularly effective as is molten potassium pyrosulfate

$$TiO_2 + 2Cl_2 \rightleftharpoons TiCl_2 + O_2$$

2.2 Titanate nanotubes

Titanium dioxide (TiO_2) is an exceptional material that has many promising applications as a catalyst, catalyst support, photocatalysis, solar cells, and sensors [6-9, 12-14]. A main limitation to the use of TiO_2 obtained by conventional methods is its low surface area. There are some ways to be studied for obtaining TiO_2 with larger surface area. Recently, titanate nanotubes, nanobelts, nanowires and nanorods have received much attention because of the wide applications and relatively simple preparation procedures needed to fulfil the requirements of various applications. One-dimensional single-crystalline Ti-O based nanomaterials have properties that compare with nanoparticles titania but possess a high surface-to-volume ratio as well [13].

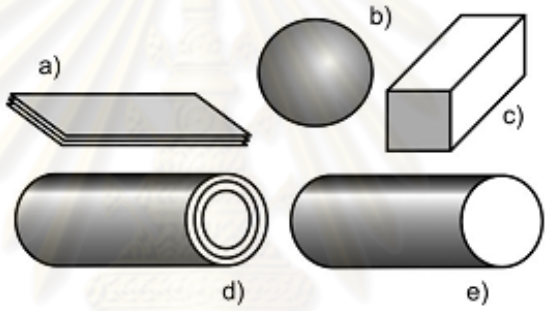

Figure 2.2 Typical morphologies of elongated titanate nanostructures: (a) sheets, (b) spheroids, (c) rectangular-section fibers, (d) multiple-wall nanotubes and (e) circular-section rods [14].

2.2.1 Synthesis method

Over the past few years, many methods have been developed for the successful fabrication of one-dimensional TiO_2 nanomaterials, including the hydrothermal method, the sol-gel method, template-based synthetic approaches and electrochemical synthesis. TiO_2-based nanotubes were first reported by Hoyer via the template-assisted method. There after, electrochemical anodic oxidation and hydrothermal treatment succeeded in fabricating TNTs. Each fabrication method can have unique advantage sand functional features and comparisons among these three approaches have been compiled in Table 2.2 Regarding the template-assisted method, anodic aluminum oxide (AAO) nanoporous membrane, which consists of an array of

parallel straight nanopores with uniform diameter and length, is usually used as template. The scale of TNTs can be moderately controlled by applied templates. However, the template-assisted method often encounters difficulties of prefabrication and post-removal of the templates and usually results in impurities. Concerning electrochemical anodic oxidation, the self-assembled TiO_2 nanotubes (π-TiO_2) with highly ordered arrays was discovered by Grimes' group, and the method is based on the anodization of Ti foil to obtain nanoporous titanium oxide film. They also demonstrated the crystallization and structure stability of π-TiO_2. The comprehensive reviews associated with the fabrication factors, characterizations, formation mechanism, and the corresponding applications of TiO_2-based nanotubes arrays have been also conducted by Grimes' group. These methods, other than the hydrothermal process, are either not suitable for large scale production or not able to yield very low dimensional, well separated, crystallized nanotubes. The demonstrated architecture of TiO_2-based nanotubes constructed via the hydrothermal treatment is capable of good crystalline formation and establishment of a pure-phase structure in one step in a tightly closed vessel.

Among the aforementioned fabrication approaches, both electrochemical anodic oxidation and hydrothermal treatment received wide investigation, owing to their cost-effective, easy route to obtain nanotubes, and the feasibility/availability of wide spread application.

Table 2.2 Comparisons of current methods in titanate nanotubes fabrication [9]

Fabrication method	Advantages	Disadvantages
Template-assisted method	- The scale of nanotube can be moderately controlled by applied template	- Complicated fabrication process - Tube morphology maybe destroyed during fabrication process
Electrochemical anodic oxidation method	- More desirable for practical applications - Feasible for extensive application - Ordered alignment with high aspect ratio	- Mass production is limited - Highly expense of fabrication apparatus
Hydrothermal method	- Easy route to obtain nanotube morphology - Feasible for extensive applications	- Long reaction duration is needed - Highly concentrated NaOH must be added

For hydrohermal method, Kasuga et al. first discovered this route for the synthesis titanium oxide nanostructures having a tubular shape in 1998 [15]. The search for nanotubular materials was inspired by the discovery of carbon nanotubes by Iijima et al. in 1991. The TiO_2 nanotubes have a large specific surface area of ~ 400 m^2 /g.

2.2.2 Structure

Ti-O based nanotubes are thought to be caused by scrolling of an exfoliated TiO_2-derived nanosheet into a hollow multiwall nanotube with spiral cross section. Unlike carbon nanotubes produced by the catalytic pyrolysis of hydrocarbons, titania nanotubes produced via the alkaline hydrothermal method have never been observed in single layer form. All reports of TiO_2 nanotubes describe the samples as multilayer-

walled nanotubular structures. The number of layers varies from two to ten. They are open-ended with several wall layers on both sides [13].

Up to now, several possible crystal structures of nanotubular products from the alkaline hydrothermal treatment of TiO_2 have been proposed, including hydrogen titanate $H_2Ti_3O_7$, orthorhombic titanates $Na_2Ti_2O_4(OH)_2$, tetratitanates $H_2Ti_4O_9$, and monoclinic TiO_2-B [13, 14, 16]. The exact determination of crystal structures of nanotubes is still incomplete because of several intrinsic difficulties posed by the nanostructures, including their small crystallite size and the wrapping of the structures along a certain crystallographic axis, both resulting in broadening of the diffraction signals. The low weight of hydrogen atoms also results in difficulties in locating their precise positions and population inside the crystals.

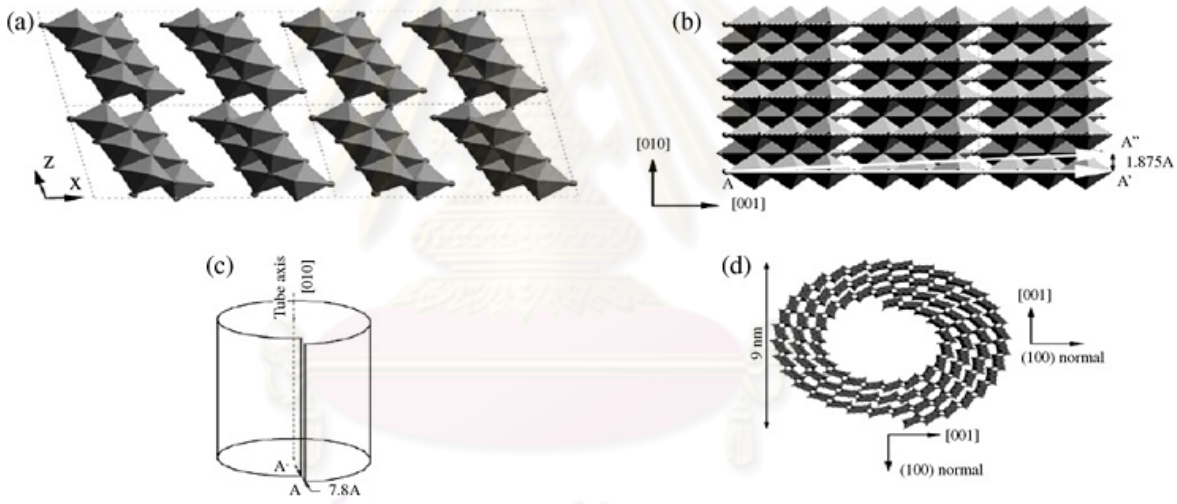

Figure 2.3 Structure models of $H_2Ti_3O_7$ (a) 2×2 unit cells on the [010] projection and (b) a layer of $H_2Ti_3O_7$ on the (100) plane from which the nanotube is constructed, (c) the introduction of a displacement vector AA' when wrapping up a sheet to form a scroll-type nanotube and (d) the structure of trititanate nanotubes [9].

2.2.3 Mechanism of titanate nanotube formation by hydrothermal method

Several researchers have studied the mechanism of titanate nanotubes formation by using both theoretical and experimental. There is a general agreement that the reaction proceeds through several stages [11, 13, 14, 17]:

1. Slow dissolution of raw TiO_2 accompanied by epitaxial growth of layered nanosheets of sodium titanates.
2. Exfoliation of the nanosheets
3. Folding of the nanosheets into tubular structures (seeds).
4. Growth of the nanotubes along the axis.
5. Exchange of sodium ions by protons during washing and separation of nanotubes.

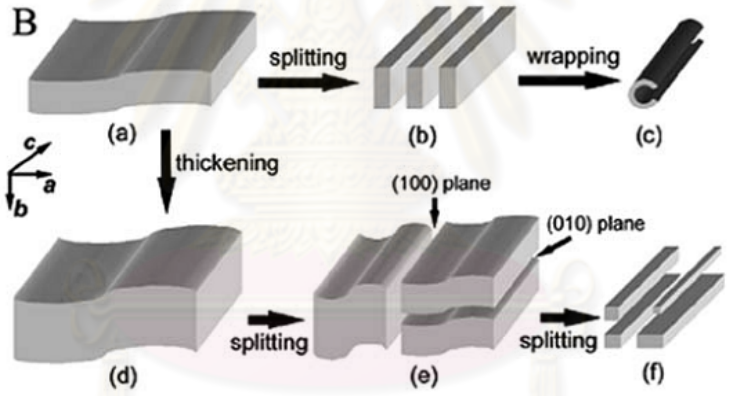

Figure 2.4 Schematic drawings depicting the formation process of $H_2Ti_3O_7$ nanotubes and nanowires [13]

2.3 Palladium metal

Palladium as a group VIII noble metal has unique catalytic properties in homogeneous and in heterogeneous reactions. In heterogeneous catalysis palladium is used for oxidation and hydrogenation reactions. One of the most remarkable properties of palladium is the ability to dissociate and dissolve hydrogen. Atomic hydrogen occupies the octahedral interstices between the Pd atoms of the cubic-closed packed metal. Palladium can absorb up to 935 times of its own volume of hydrogen.

Table 2.3 Some physical properties of palladium.

Atomic number	46
Atomic weight	106.42
Atomic diameter	275.2 pm
Melting point	1827 K
Crystal structure	cubic closed packed
Electron configuration	$[Kr]4d^{10}$

Palladium can be used for hydrogenation of unsaturated hydrocarbons. Palladium shows the highest selectivity of group VIII metals in heterogeneously catalyzed semi-hydrogenation of alkynes and dienes to the corresponding alkenes [2-4]. Activity of palladium for hydrocarbon hydrogenation is based on the ability for the dissociative adsorption of hydrogen and chemisorption of unsaturated hydrocarbons. Palladium shows a strong deactivation behavior because of hydrocarbon and carbon deposits. For heterogeneous system in particular catalyst performance is strongly influence by, firstly the ability to get reactant to the active sites, then to establish the optimum hydrogen-to-hydrocarbon surface coverage, and, finally, the rapid removal of the hydrogenated products.

2.4 Hydrogenation reaction

Catalytic hydrogenation reaction is a well known versatile reaction widely used in organic synthesis. Many functional groups contained in organic substrates can be hydrogenated to produce several useful compounds which has been used for wide applications such as monomers for production of various polymers, fats and oil for producing edible and no edible products, and intermediates used in pharmaceutical industry. Hydrogenation processes are often carried out in a small scale in batch reactor. Batch processes are usually most cost effective since the equipment need not to be dedicated to a single reaction. Typically the catalyst is powdered and slurried with reactant; a solvent is usually present to influence product selectivity and to adsorb the reaction heat liberated by the reaction. Since most hydrogenations are

highly exothermic, careful temperature control is required to achieve the desired selectivity and to prevent temperature runaway.

Selective hydrogenation of alkynes is an addition of hydrogen to a carbon-carbon triple bond in order to produce only alkenes product. The overall effect of such an addition is the reductive removal of the triple bond functional group. The simplest source of two hydrogen atoms is molecular hydrogen (H_2), but mixing alkynes with hydrogen does not result in any discernable reaction. However, careful hydrogenation of alkynes proceeds exclusively to the alkenes until the former is consumed, at which point the product alkenes is very rapidly hydrogenated to an alkanes. Although the overall hydrogenation reaction is exothermic, high activation energy prevents it from taking place under normal conditions. This restriction may be circumvented by the use of a catalyst, as shown in the following diagram.

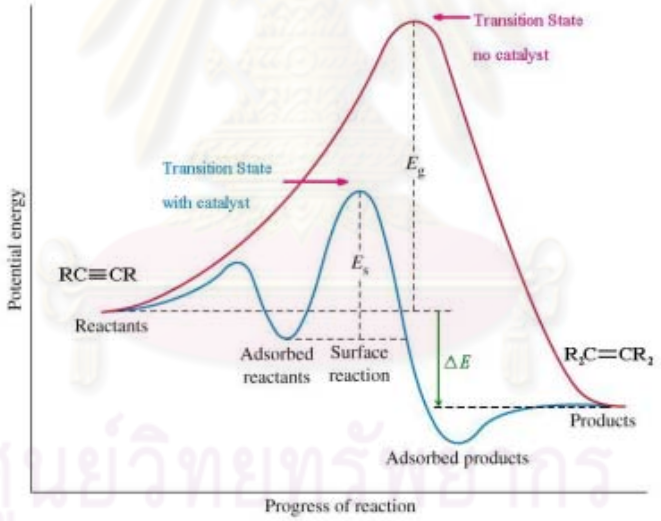

Figure 2.5 Diagram of hydrogenation reaction

Selective hydrogenations of alkynes to alkene are the reactions which take place on the surface of the metal catalyst. The mechanism of the reaction can be described in four steps:

Step 1: Hydrogen molecules react with the metal atoms at the catalyst surface. The relatively strong H-H sigma bond is broken and replaced with two weak metal-H bonds.

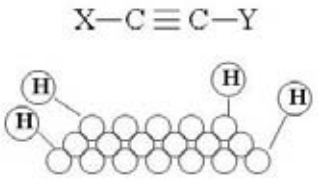

Step 2: The pi bond of the alkyne interacts with the metal catalyst weakening the bond. A hydrogen atom is transferred from the catalyst surface to one of the carbons of the triple bond.

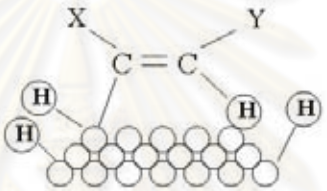

Step 3: The pi bond of the alkyne interacts with the metal catalyst weakening the bond. A second hydrogen atom is transferred from the catalyst surface forming the alkene.

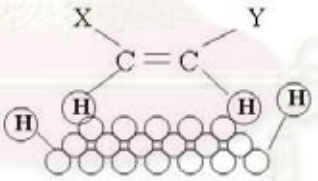

Step 4: The alkene is released from the catalyst's surface allowing the catalyst to accept additional hydrogen and alkene molecules.

CHAPTER III

LITERATURE REVIEWS

3.1 Synthesis of titanate nanotubes

3.1.1 Synthesis parameters

Hydrothermal method has received attention for preparation titanate nanotubes due to its simple procedure and low production cost [9]. In 1998, Kasuga *et al*. [15] first discovered the alkaline hydrothermal route for the synthesis of titanium oxide nanostructures having a tubular shape. Needle-shaped TiO_2 crystals (anatase phase) with a diameter of ≈ 8 nm and a length of ≈ 100 nm were obtained when sol-gel derived fine TiO_2-based powders were treated with a 5-10 M NaOH aqueous solution for 20 h at 110 °C. The derived TiO_2 nanotubes have a large specific surface area of ~ 400 m^2/ g.

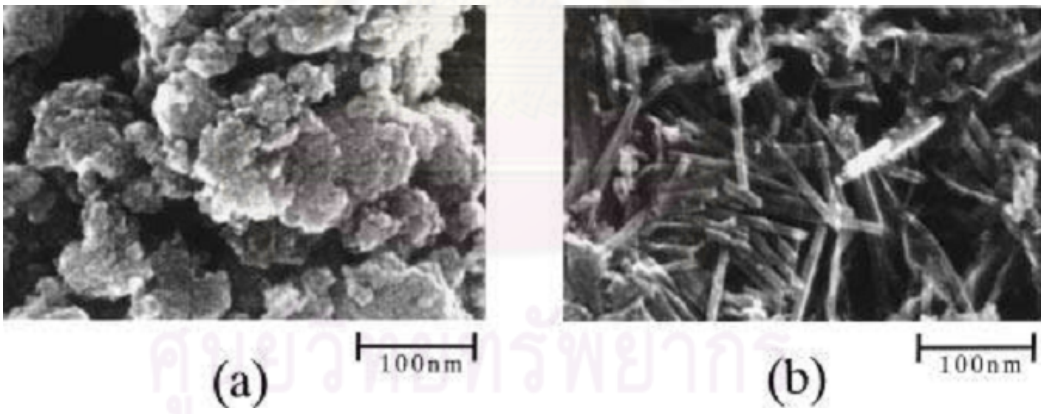

Figure 3.1 SEM photographs of (a) $80TiO_2$ $20SiO_2$ (in mol %) powders prepared by heating at 600 °C and (b) the powders obtained by treating the powders in part a chemically with 10 M NaOH aqueous solution for 20 h at 110 °C [15]

Following the discovery of titanate nanotubes by Kasuga *et al.*, many investigations have been carried out on the formation, morphology, and structure of titanate nanotubes. It has been found that the hydrothermal temperature [10, 18], treatment duration, starting materials [19, 20], ratio of titania and NaOH [18], and

concentration of base solution [21] have strong effects on controlling the phase and morphology of the resulting materials. For the effect of the hydrothermal temperature on morphologies of titanate, many experiments have been performed. It was commonly accepted that nanotubes are formed under milder reaction conditions (110-150 °C and a time period between 24 and 72 h) in the concentration of alkaline solution by the rolling up of exfoliated titanate sheets. At a lower treatment temperature (lower than 120 °C), a large amount of residual TiO_2 particles can be found in the obtained products. Hyung-Kee Seo *et al*. [10] investigated the preparation of titanate nanotubes from TiO_2 via hydrothermal method. TiO_2 powders were treated with 10 M NaOH solution in a Teflon-lined autoclave at various reaction temperatures ranging from 70 to 150 °C over 48 h. As can be seen in Figure 3.2, after hydrothermal treatment at 70 °C, the spherical particles undergo delaminating process due to attack of excess sodium cations, to produce two-dimensional nanosheets. At 90 °C, nanosheet and fiber-like mixed phase materials are observed. Increasing reaction temperature to 110 °C, the nanosheets completely transform to tubular structure which diameter ~ 10-20 nm and lengths few hundreds of nanometers. Hydrothermal synthesis at 150 °C results in improved crystallinity of the tubes. They suggested that reaction temperature is a key factor in determining titanate morphology. In other reported, such as Mao, Y. [22] synthesized titanate nanotubes at 110-190 °C. The result from HRTEM showed that the titanate prepared at 120 °C revealed that nanotubes normally consisted of 3-5 layers. The nanotubes have lengths in the range of several hundred nanometers, outer diameters of ~ 7-10 nm, and inner diameters of 3-5 nm.

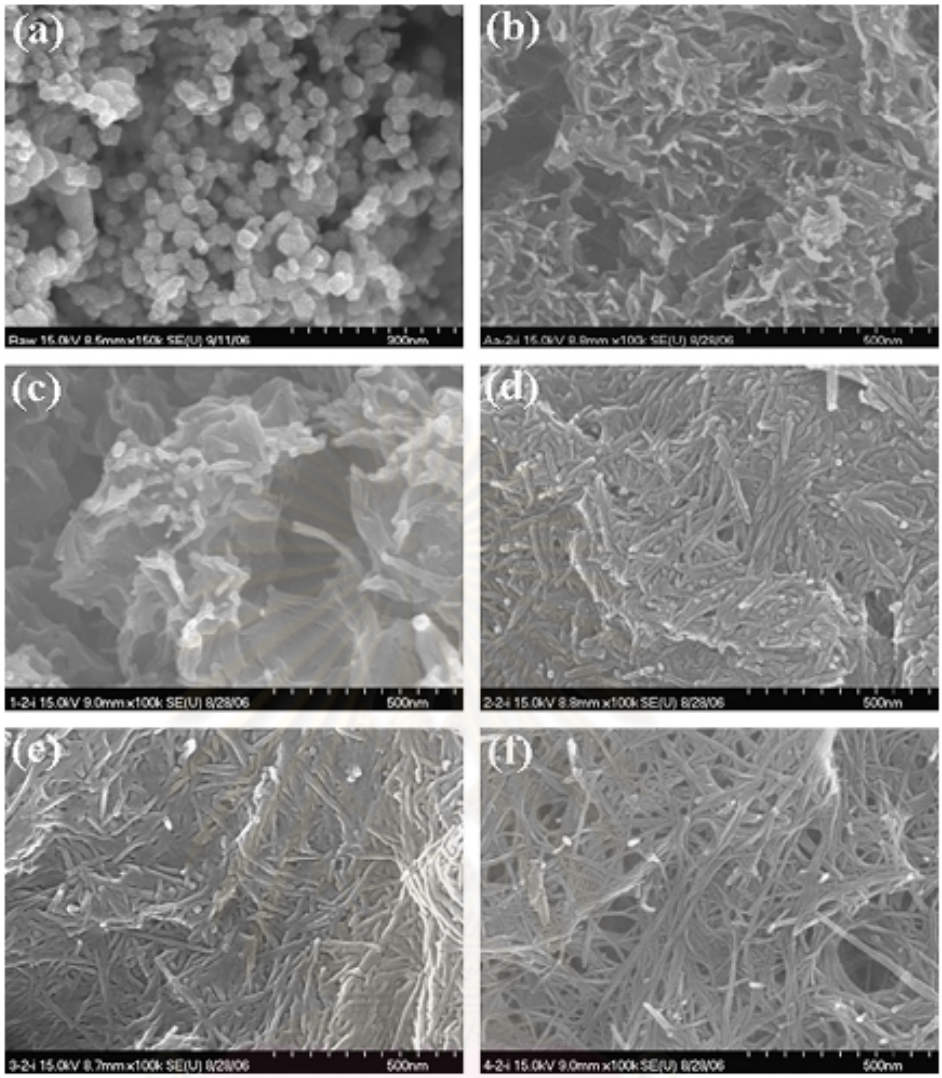

Figure 3.2 High-resolution micrographs of (a) starting material (b) and hydrothermally synthesized materials at various reaction temperatures: 70 °C, (c) 90 °C, (d) 110 °C, (e) 130 °C, and (f) 150 °C

A higher treatment temperature (temperatures higher than 170 °C) and longer duration hydrothermal treatment promote unidirectional crystal growth, leading to nanowires, nanowhiskers or nanofibers. Bavykin, D. V. *et al.* [23] studied the effect of hydrothermal conditions on the mesoporous structure of TiO_2 nanotubes to explained the mechanism of tubes formation. The preparation was performed by mixed anatase TiO_2 with 10 M NaOH and heated at 120-190 °C. A mechanism of TiO_2 nanotube formation has been proposed, which includes the stage of multilayered titanate nanosheet wrapping. The driving force for curving of nanosheets is believed to be the mechanical stress due to the imbalance in the width of layers in the multilayered

nanosheets. The titanate nanofibers can be form at 190 °C. This formation temperature consistent with Mao, Y. [22] report. They synthesized titanate nanotubes at 110-190 °C. At temperature 180 °C, results in the formation of titanate nanowires with a few microns long and ~ 65-400 nm wide.

In addition, the effect of duration treatment and NaOH to TiO_2 ratio were investigated by Sreekantan, S. *et al.* [18]. The titanate nanotubes were synthesized by using commercial TiO_2 as starting material. Titanate nanotubes with 10 nm diameter was formed for NaOH to TiO_2 ratio > 27 treated at 110 °C for 24 h. Increasing the synthesis temperature to 150 °C, the titanate nanotubes transformed to anatase phase and it was found minimum of 15 h is required for completing transformation from nanoparticles to nanotubular structure. The degradation of methyl orange aqueous solution was performed to evaluate the photocatalytic activity of the sample. They found that TiO_2 synthesized at 150 °C showed the best photocatalytic behavior. These due to the high surface area of the tube-like structure and the presence of anatase phase in this sample.

3.1.2 Stability of titanate nanotubes

Titanate nanotubes have poor stability in dilute inorganic acids even at room temperature, and slowly transform to rutile nanoparticles over several months. The rate of transformation depends on the nature of the inorganic acid and is correlated to the solubility of the titanates in the acid. The hydrothermal treatment in acidic conditions were investigated by Murakami, N. *et al*. [24]. They reported that hydrothermal treatment in the presence of Cl^- at high temperature accelerated the transformation of titanate nanotubes to a rutile phase. Bavykin *et al*. [25] reported the nanotubes were stable and minimal morphological changes occurred in pure water and basic (0.1 mol dm^{-3} NaOH) solutions. In 0.1 mol dm^{-3} H_2SO_4, suspended titanate nanotubes slowly transform to rutile nanoparticles of ca. 3 nm size, which agglomerated into ellipsoidal particles.

Typically, the titanate nanotubes are not stable at high temperature. $H_2Ti_3O_7$ nanotubes are susceptible to lattice oxygen depletion and transform above 397 °C into complete rod-like structures. Recent systematic thermal transformation studies of

titanate nanotubes have revealed that annealing them in the temperature range 120-400 °C results in slow dehydration of the initial nanotubular $H_2Ti_3O_7$ to form nanotubular TiO_2 (B) accompanied by a decrease in interlayer spacing of the nanotubewalls. A further increase in temperature results in the transformation of nanotubular TiO_2 (B) to anatase nanorods, which is accompanied by a loss of tubular morphology. Nanofiber titanates can transform to nanofibrous TiO_2 (B) at 400 °C, followed by transformation to nanofibrous anatase at 700 °C and then completely transformed to submicron rod-like structure of rutile at 1000 °C. The formation of anatase nanofibers is also possible by using hydrothermal post-treatment of the titanate nanofibers in water at 150 °C. Compared with nanotubes, Riss *et al*. [26] found that nanowires have higher thermal stability.

Sreekantan, S. [18] reported the transformation after annealing titanate nanotubes, the sample undergo dehydration and form anatase phase at 300 °C and the degree of crystallinity was improved with increasing annealing temperature. Besides, the sintegration of the nanotubes was observed at 500 °C and the structure completely transformed to nanoparticles at 600 °C.

3.2 Synthesis of palladium nanoparticles

Several methods have been employed for preparation of Pd catalysts. The simplest and most common procedure is impregnation method. Advantages of the impregnation include its relative simplicity, rapidity and capability for depositing the precursor at a high metal loading. A principle disadvantage is that sometimes material is nonuniformly deposited along pores and through the pellet; another is the tendency for deposited base metal precursors to be oxidized in the aqueous solution to oxides that interact strongly with alumina or silica supports and which are difficult to reduce. The reduction-by-solvent method is an interesting one because uniform small Pd nanoparticles and higher dispersion can be obtained. According to Domínguez-Domínguez S., *et al.* [27], they prepared the stable mono and bimetallic colloids nanoparticles by reduction by solvent process. The metallic nanoparticles were prepared with different compositions (i.e., Ni-Pd, Fe-Pd, Mg-Pd, Pd, and Pt) and metallic ratios, and anaverage size of about 2 nm. Metallic species were used as homogeneous phase in the selective hydrogenation of phenylacetylene to styrene in

liquid phase under very mild conditions (1 bar H_2 pressure and T = 50°C). They found that the catalysts prepared show high selectivity and activity toward styrene at very high loadings of phenylacetylene. In addition, the prepared metallic nanoparticles are very interesting compared with other homogeneous catalysts especially in terms of selectivity, reaching values very close to 97 %. An interesting advantage of using bimetallic nanoparticles is to bring down the cost of production by using fewer amounts of noble metal precursors. In addition, Domínguez-Domínguez S., *et al.* [28] studied palladium colloids supported on difference three types of carbon supports: multiwall carbon nanotubes (NTs), carbon black (CB), and an activated carbon (AC). The colloidal Pd nanoparticles were synthesized by reduction by solvent method. These catalysts were tested in a hydrogenation reaction of phenylacetylene. The AC provokes a Pd particle agglomeration, and the catalyst has the lowest activity and selectivity. The highest selectivity is obtained for the Pd/NT catalyst.

Figure 3.3 TEM image of a purfied Pd colloid synthesized by reduction by solvent method [27]

The heterogeneous catalyst (palladium nanoparticles) supported on inorganic materials such as γ-alumina, β-zeolite, MCM-41, and Al-MCM-41 in the liquid-phase semihydrogenation of phenylacetylene under very mild conditions were investigated

by Domínguez-Domínguez, S. *et al.* [29]. MCM-41 and Al-MCM-41 used the one alternative method to deposit the Pd nanoparticles called simultaneous synthesis (s.s.). The Pd-supported catalysts exhibited very similar catalytic activity (high selectivity toward styrene as same as previous work). All of the catalysts had very high selectivity toward styrene (around 96 %) after total conversion. They found that no Pd leaching from the samples occurred during the catalytic reaction.

3.3 Titanate nanotubes supported Pd in the hydrogenation reaction

The properties of elongated morphology, high surface area render nanostructure titanate promising for many applications such as photocatalysis, hydrogen production and storage, solar cells, and catalyst support. Titanate nanotubes are used in heterogeneous catalytic process as supports. The high surface area of the support facilitates a high dispersity of the catalyst, while an open mesoporous structure provides an efficient transport of reagents and products. The selective hydrogenation of o-chloronitrobenzene (o-CNB) over Pd supported titanate nanotubes catalyst was investigated by Sikhwivhilu, L. M. *et at.* [30]. Titanate nanotube was synthesized by treating P-25 Degussa TiO_2 with a concentrated (18 M) KOH solution. The vapour-phase hydrogenation of o-CNB was performed in ethanol at 523 K and atmospheric pressure over a Pd/TiO_2 derived nanotube catalyst (Pd/TiO_2-M). The result showed that Pd/TiO_2-M gave complete conversion (100 %) of o-CNB with the selectivity to ortho-chloroaniline (o-CAN) of 86 % which higher than P-25 TiO_2 commercial supported Pd. The stability of the Pd/TiO_2-M catalyst was tested over 5 h during which time the conversion slowly dropped to 80 % (selectivity 93 %) due to catalyst poisoning. The TPR analysis revealed the existence of a strong palladium-support interaction and this was found to be crucial to the overall activity of the catalyst. In addition, Sikhwivhilu, L. M. *et at*. [31] synthesized nanotubular titanates by using a commercial TiO_2 (Degussa P25 containing anatase and rutile phases) and a base (KOH) solution at 120 $^{\circ}$C for 20 h. Prior to the removal of KOH, the samples of TiO_2 were aged for three different time intervals (0, 2, and 61 days). Pd was loaded to the titanate support by wet impregnation with 1 wt% Pd content. The catalytic performance was tested in the gas-phase phenol hydrogenation reaction within the temperature range of 165-300 $^{\circ}$C under atmospheric pressure. It was found that aging for 2 days showed the best activity (conversion 97 %) and total selectivity to

cyclohexanone (99 %). The Pd (II) and Pd (0) catalysts supported on to titanate nanotubes ($H_2Ti_3O_7$) prepared by an ion-exchange technique was studied by Murciano, L. T. *et al.* [32]. The titanate nanotubes prepared by hydrothermal at 140 °C. The catalysts were characterised by narrow size distribution of metal nanoparticles on the external surface of the nanotubes. Pd (II) catalysts show high selectivity toward double-bond migration reaction versus hydrogenation in linear olefins. The Pd (II) was shown to be rapidly reduced to Pd (0) by appropriate choice of solvent. Prereduced Pd (0) catalysts were found to be less active toward double-bond migration and more selective toward hydrogenation.

3.4 Supported Pd catalysts in liquid-phase hydrogenation

The selective hydrogenation of alkynes to alkenes is an important reaction in the synthesis of biologically active compounds such as insect sex pheromones (pestcontrol) and vitamins [3]. Palladium (Pd) is the most selective of the noble metal catalysts for alkyne semihydrogenation with respect to over all alkene formation. The classic Lindlar catalyst, consisting of metallic Pd on calcium carbonate support modified with lead (II) acetate, is the well known commercially available catalyst for such reaction. The high activity and selectivity maybe obtained over other catalyst systems such as Pd/TiO_2 [4], Pd/SiO_2 [1, 3, 33], and Pd/Al_2O_3 [34]. Somboonthanakij *et al.* [3] investigated the catalytic behavior of 1-heptyne hydrogenation over Pd/SiO_2 catalyst. The catalyst was prepared by one-step flame spray pyrolysis (FSP) which Pd loading 0.5-10 wt%. The selective hydrogenation of 1-heptyne was carried out under liquid-phase at 30 °C, 1 bar. It was found that the conversion of 1-heptyne increased from 42 to 75 % as Pd loading increased from 0.5 to 5 wt% and remained relatively constant when Pd loading was increased to 10 wt%. The selectivities for 1-heptene were in the range of 92-95 % for all the Pd/SiO_2 catalysts. In addition, the flame-made catalysts were compared with Pd/SiO_2 catalyst prepared by incipient wetness impregnation on a commercial SiO_2 support. For similar Pd loading, the catalytic activity of the flame-made catalyst was higher than impregnation.

Lederhos, C. R. *et al.* [34] studied the catalytic behavior of Pd supported on γ-Al_2O_3 and on an activated pelletized carbon in the selective hydrogenation of 1-heptyne to 1-heptene. Catalysts were prepared by incipient wetness technique with

5 wt% Pd. Under the same operating conditions, Pd/Al_2O_3 also presents a better performance than the classic Lindlar catalyst. The reduction and operating temperatures were found to play an important role in the catalytic behavior of the catalysts studied. The XPS results show that palladium in Pd/Al_2O_3 and Pd/C is electron-deficient. With in certain limits, the electron-deficient Pd species do not favor the further hydrogenation of 1-heptene to heptane, thus raising the selectivity to 1-heptene. The differences observed in the catalytic behavior of Pd/Al_2O_3 and Pd/C could be attributed, at least partially, to the differences in the support porosity.

Weerachawanasak, P. *et al.* [35] investigated the liquid-phase semihydrogenation of phenylacetylene on a series of solvothermal-derived nano-TiO_2 supported Pd catalysts with various TiO_2 crystallite sizes in the range of 9-23 nm. As revealed by CO chemisorption and transmission electron microscopy, all the catalysts exhibited strong metal-support interaction (SMSI) when reduced at 500 $^{\circ}$C. The catalysts with SMSI show remarkably high catalytic performance in terms of both hydrogenation activities (turnover frequencies 9.1-21.4 s^{-1}) and moderate-high selectivities to styrene (86-90 %) at complete conversion of phenylacetylene. Without SMSI effect (the catalysts reduced at 40 $^{\circ}$C), styrene selectivity and catalytic activity depended largely on the Pd particle size in which small Pd particles (formed on small crystallite size TiO_2 supports) exhibited lower phenylacetylene conversion and poor styrene selectivity.

Mekasuwandumrong, O. *et al.* [4] studied liquid-phase selective hydrogenation of 1-heptyne on the Pd/TiO_2. The Pd/TiO_2 nanoparticles synthesized by one-step flame spray pyrolysis (FSP) with Pd loadings 0.5-10 wt% showed good catalytic performances. Higher selectivities to 1-heptene at complete conversion of 1-heptyne were obtained on the FSP-derived catalysts compared to the ones prepared by conventional impregnation of palladium on the FSP-synthesized and the commercial P-25 TiO_2 supports. The XRD peak corresponding to PdO One-Step Flame Spray Pyrolysis phase was evident for flame-and impregnation-made 5 and 10 wt% Pd/TiO_2 catalysts. For those with Pd loading $\leq$ 2 wt%, the Pd/PdO particle size maybe smaller than XRD detect ability limit so that the corresponding XRD peaks were not apparent. The improved catalytic properties of Pd/TiO_2 were attributed to a stronger interaction/

an intimate contact between the very fine Pd particles and the TiO_2 support obtained via one-step FSP synthesis.

Panpranot, J. *et al.* [36] studied liquid-phase hydrogenation of cyclohexene under mild conditions on Pd/SiO_2 in different organic solvents (benzene, heptanol, and NMP), under pressurized carbon dioxide, and under solvent less condition were investigated and compared. In the cases of using organic solvents, the hydrogenation rates depended on polarity of the solvents in which the reaction rates in high polar solvents such as heptanol and NMP were lower than that in a non-polar solvent. Hydrogenation rates were much higher when the reactions were performed under high-pressure CO_2 or under solvent less condition. The use of high-pressure CO_2 can probably enhance H_2 solubility in the substrate resulting in a higher hydrogenation activity. However, metal sintering and leaching in the presence of high-pressure CO_2 were comparable to those in organic solvents.

Panpranot, J. *et al.* [33] studied the differences between Pd/SiO_2 and Pd/MCM-41 catalysts in liquid phase hydrogenation of 1-hexene. SiO_2-small pore, SiO_2-large pore, MCM-41-small pore, MCM-41-large pore were used as support. The catalysts were prepared by incipient wetness impregnation. The reaction was carried out at 25 $^{\circ}$C and 1 atm in a stainless steel Parr autoclave. The results showed that the characteristics and catalytic properties of the silica supported Pd catalysts were affected by type of silica, pore size and pore structure. The catalyst activities were found to be merely dependent on the Pd dispersion, which as a function of the support pore structure. Among the four types of supported Pd catalysts, Pd/MCM-41-large pore showed the highest Pd dispersion and the highest hydrogenation rate with the lowest amount of metal loss.

3.5 Comments on previous studies

From the previous studies, hydrothermal method is suitable route for synthesis of titanate nanotubes. Reaction temperature, reaction time, concentration of NaOH, and size of raw TiO_2 powder were considered as the predominant factors in the formation of nanotubes. However, the effects of quenching and annealing treatments on the properties of titanates have not been reported to much of a degree. In the

liquid-phase selective alkyne hydrogenation, supported palladium catalysts present the best performance in terms of catalytic activity and selectivity towards alkenes. Several methods have been employed for preparation of Pd catalysts. The reduction-by-solvent method is an interesting one because uniform small Pd nanoparticles can be obtained. The common supports used for Pd catalysts in the selective alkyne hydrogenation include SiO_2, Al_2O_3, and TiO_2. However, there are no reports on the use of Pd nanoparticles supported on titanate nanotubes in the liquid-phase hydrogenation. Thus, the purpose of this study is to investigate the preparation conditions on the formation and morphology of titanate nanotubes and nanowire and their applications as Pd catalyst supports in the liquid-phase selective hydrogenation of 1-heptyne.

CHAPTER IV

EXPERIMENTAL

This chapter describes the experimental procedure used in this research which can be divided into three sections. The first part explains support and catalyst preparation. The reaction study in liquid phase hydrogenation of heptyne is explained in second part. Finally, the properties of the catalyst characterized by various techniques are discussed in section three.

4.1 Catalysts preparations

4.1.1 Materials

The chemicals used in this study are specified as follows in Table 4.1.

Table 4.1 Chemical used for synthesis Pd nanoparticles and titanate supports

Chemical	Supplier
Titanium dioxide (TiO_2), anatase ≥99%	Sigma
Sodium hydroxide, ≥99%	Merck
Ethylene glycol, ≥ 99%	Sigma-Aldrich
Palladium(II)acetate	Sigma-Aldrich
1, 4-dioxane	Sigma-Aldrich
Poly (n-vinylpyrrolidone)	Sigma-Aldrich
Methanol	Merck
Ethanol	Merck
Acetone	-
De-ionized water	-

4.1.2 Preparation of titanate supports

Preparation of titanate nanotubes was carried out by hydrothermal method using anatase TiO_2 as starting material. First, 1.5 g of TiO_2 powder was mixed with 40 ml of 10 M NaOH and the mixture was sonicated for 10 min. Thereafter the mixture was transferred to a Teflon-lined stanless steel autoclave, and heated at various reaction temperatures ranging 110-200 °C for 24 hours in oven. After hydrothermal reaction, the autoclave was cooled to room temperature by natural cooled down. By the other condition, the autoclave was cooled by quenching in ice bath. Then the sample was washed with 0.1 M HCl for several time and followed by deionized water until pH value approached deionized water. Finally, the sample was dried at 110 °C for 24 h. The dried powder was annealed at 400, 500, and 600 °C for 1 h.

4.1.3 Preparation of Pd nanoparticles

The Pd nanoparticles were synthesized by using reduction by solvent method in accordance with the method described by Dominguez S. *et al*. [28]. Ethylene glycol was used to reduce the Pd precursor. The experimental were performed under an Ar atmosphere by mean of a Schlenk system, and the three-necked, round bottom flask were used in the experiment.

Solution A composed of 0.800 g of poly-n-vinyl pyrrolidone and 120 mL of anhydrous ethylene glycol under stirring and heated at 80 °C for 3 h. Then, the solution was cooled to 0°C.

Solution B included 0.2245 g of palladium (II) acetate and 50 mL of 1, 4-dioxane. The solution was vigorous stirring for 2 h.

Solution B was poured into solution A under stirring and adjusted the pH to 9-10 by dropwise 1 M NaOH solution. The solution was heated at 100 °C under vigorous stirring. After that, the solution was dark brown in color and non transparent, indicating that the colloid was formed. The heating was continued for 2 h and then, cooled to room temperature.

The prepared Pd nanoparticles colloids were treated with large excess of acetone in order to removed the polymeric protecting agent by centrifugation several times. Finally, the Pd colloid was redispersed in a certain volume of methanol.

4.1.4 Preparation of titania and titanate supported Pd catalysts

The Pd nanoparticles were supported on the titania and titanate using wet impregnation method. First, the appropriate volume of Pd nanoparticles/methanol dispersion was mixed with the supports. All catalysts were prepared so as to have a final catalyst loading of ca. 1 wt%. The mixture was gentle stirred at room temperature for 3 days and heated at 60 $^{\circ}$C for the purpose of removed the methanol solution. The collected solid was washed with ethanol and water (50/50% V/V) for several times. Finally, the catalysts were dried overnight.

For impregnation catalyst, the catalyst was prepared by wet impregnation method. Palladium chloride solution was used as a precursor for final loading of ca. 1 wt%. The support and precursor was stirred. Then, the catalysts were dried at 110 $^{\circ}$C overnight. Finally, the catalysts were calcined in air at 450 $^{\circ}$C for 3 h.

In addition, the effect of Pd loading method was investigated by comparing sonication to those with were stirred.

4.2 The reaction study in liquid-phase hydrogenation of 1-heptyne

4.2.1 Chemicals

The chemicals used in liquid-phase hydrogenation of 1-heptyne are specified as follows in Table 4.2.

Table 4.2 Chemical used for liquid-phase hydrogenation of 1-heptyne

Chemical	Supplier
1-Heptyne, 98%	Aldrich
1-Heptene	TCI
Heptane	Wako
Toluene, ≥ 99.9%	Merck

4.2.2 Instrument and apparatus

The main instrument and apparatus are explained as follow:

The autoclave reactor

The 50 ml stainless steel autoclave was used as reactor. Hot plate stirrer with magnetic bar was used to heat up the reactant and to ensure that reactant and catalyst were well mixed.

Gas chromatography

A gas chromatography equipped with flame ionization detector (FID) with GS-alumina capillary column was used to analyze the feed and product.

Table 4.3 Operating condition for gas chromatograph

Gas chromatograph	Shimadzu GC-14B
Detector	FID
Packed column	GS-alumina (length = 30 m, I.D.= 0.53 mm)
Carrier gas	Helium (99.99 vol. %)
Make-up gas	Nitrogen (99.99 vol. %)
Column temperature	200 °C
Injector temperature	250 °C
Detector temperature	280 °C

4.2.3 Liquid-phase hydrogenation procedure

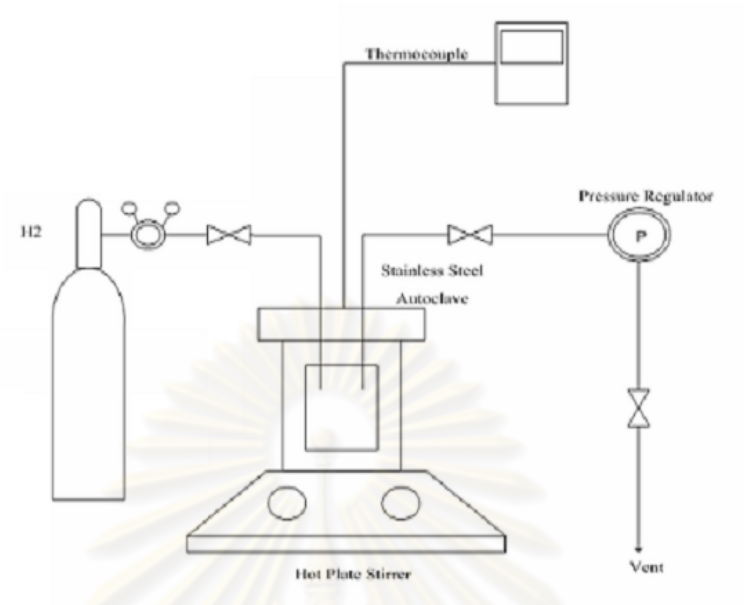

Figure 4.1 Schematic diagram of liquid-phase hydrogenation

0.2 ml of 1-heptyne and 9.8 ml of toluene were mixed in the volumetric flask. Next, the mixture and 20 mg of catalyst were introduced into the autoclave reactor. The reaction was carried out under hydrogen atmosphere at 1 atm and 30 °C. After the reaction, the vent valve was slowly opened to prevent the loss of product. Then the product was analyzed by gas chromatography with flame ionization detector (FID).

4.3 Catalyst characterization

The properties of the prepared support and catalysts were characterized by various techniques are discussed below.

4.3.1 X-ray Diffraction (XRD)

The X-ray diffraction (XRD) patterns of powder were obtained using an X-ray diffractometer SIEMENS D5000 connected with a computer with Diffract ZT version 3.3 program for fully control of the XRD analyzer. The experiments were carried out

using Ni-filtered CuKα radiation. Scans were performed over the 2θ ranges from 10° to 80°.

4.3.2 N_2 Physisorption

Specific surface area of sample was measured through nitrogen gas adsorption at liquid nitrogen temperature (-196°C) using Micromeritics ChemiSorb 2750 Pulse chemisorption System instrument. Before measurement the sample was thermally treated at 150°C for 1 h.

4.3.3 Scanning Electron Microscope (SEM)

The catalyst granule morphology and elemental distribution were obtained using a Hitachi s-3400N scanning electron microscope. The SEM was operated using the back scattering electron (BSE) mode at 20 kV. The catalysts were prepared with platinum coating prior to analysis.

4.3.4 Transmission Electron Microscopy (TEM)

The palladium nanoparticles, titanate supports, and prepared catalysts are investigate the structure, Pd particles size, and distribution of palladium on the titante support are observe using JEOL-JEM 2010 transmission electron microscope operated at 200 kV.

4.3.5 X-ray Photoelectron Spectroscopy (XPS)

The XPS spectra, the blinding energy and the composition on the surface layer of the catalysts were determined by using a Kratos Amicus X-ray photoelectron spectroscopy. The experiment was carried out of 20 mA and 12 kV, 0.1 eV/step of resolution, and pass energy 75 eV and the operating pressure approximately $1x10^{-6}$ Pa.

4.3.6 Inductive Coupled Plasma Optical Emission Spectrometer (ICP-OES)

The actual amount of the metals loading were determined by a Perkin Elmer Optima 2100DV AS93 PLUS inductive coupled plasma optical emission spectrometer. The catalysts were prepared in a solution containing 65% HNO_3, 49% HF, and 37% HCl with volume ratio 1:3:1 and were heated for increasing of dissolve its.

4.3.7 CO-Pulse Chemisorption

The active sites per gram of catalysts and the relative percentages dispersion of palladium catalyst are determined by CO-pulse chemisorption technique using Micromeritics ChemiSorb 2750 (pulse chemisorption system). Approximately 0.1 g of catalyst was filled in a U-tube, incorporated in a temperature-controlled oven and connected to a thermal conductivity detector (TCD). Helium was introduced into the reactor at the flow rate of 30 ml/min in order to remove remaining air. Prior to chemisorp, the samples were reduced in a H_2 flow rate at 50 ml/min with heated from room temperature to 40 $^{\circ}$C and held at this temperature for 2 h. Carbon monoxide that was not adsorbed was measured using thermal conductivity detector. Pulsing was continued until no further carbon monoxide adsorption was observed.

CHAPTER V

RESULTS AND DISCUSSION

This chapter presents the results with a discussion about the characteristics and the catalytic properties of titanate supports and the titanate supported Pd catalysts in the liquid-phase selective hydrogenation of 1-heptyne to 1-heptene under mild conditions (30 °C, H_2 pressure = 1 atm). The results and discussion are divided into two sections. The first section describes the characteristics of the titanate supports and the titanate supported Pd catalyst by using several techniques such as XRD, SEM, TEM, N_2 physisorption, CO-chemisorption, XPS, and ICP. The second section reports the catalytic properties of supported Pd catalysts in the liquid-phase selective hydrogenation of 1-heptyne.

5.1 Catalyst characterization

5.1.1 Characterization of titanate supports

The titanate supports were characterized by means of XRD, SEM, TEM, and N_2 physisorption in order to investigate the structure and morphology of samples.

5.1.1.1 X-Ray Diffraction (XRD)

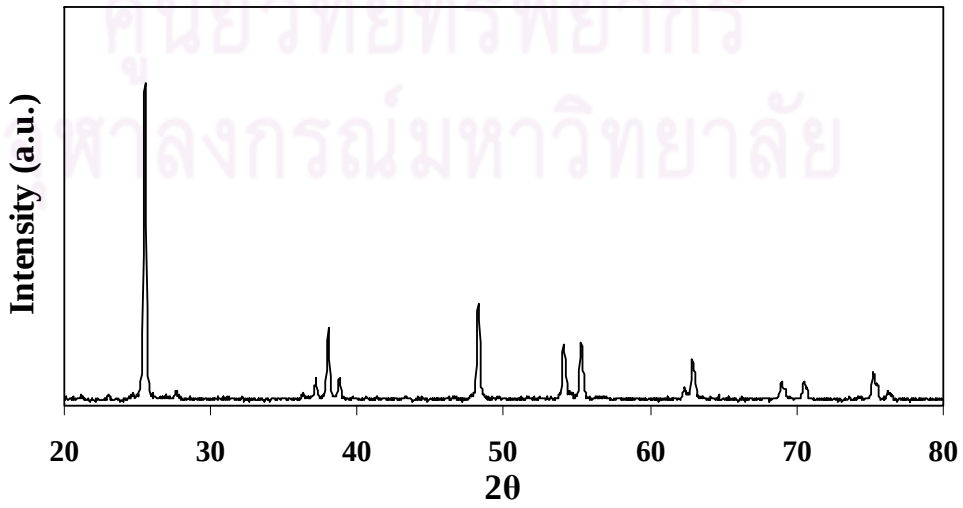

Figure 5.1 XRD pattern of commercial titania

The XRD patterns of the starting anatase TiO_2 and the samples obtained at different reaction temperatures are shown in Figure 5.1 and 5.2, respectively. The XRD pattern of the product obtained from hydrothermal synthesis at 110 °C remained anatase phase TiO_2. When the reaction temperature increased to 150 °C and 200 °C, the XRD characteristic peaks of titanate were observed. The XRD pattern of obtained materials shows two main peaks at $2\theta \approx 24.5^o$ and 48.5^o corresponding to the reflection (100) and (200) plane of H-titanate [6].

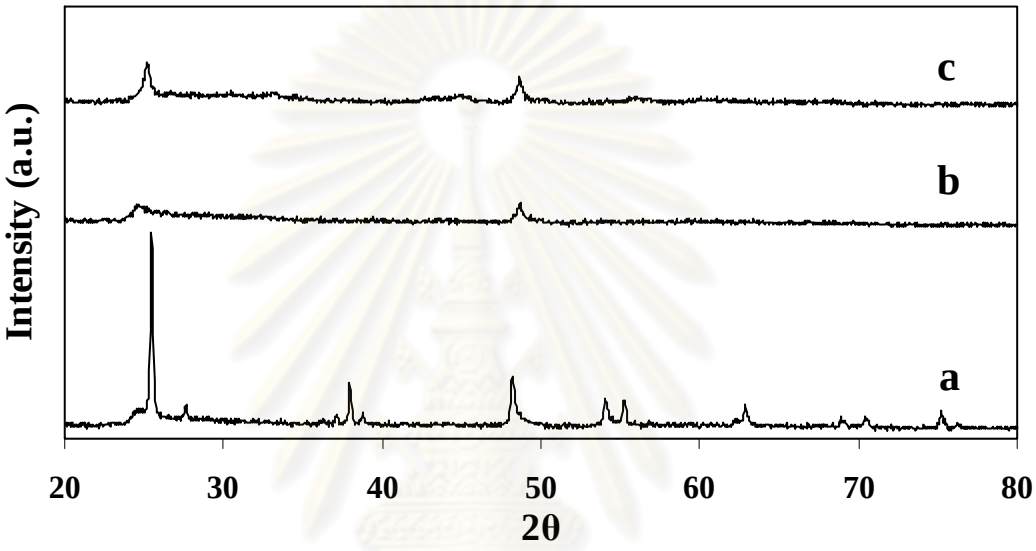

Figure 5.2 XRD patterns of the sample synthesized at different reaction temperatures: 110 °C (a), 150 °C (b), and 200 °C (c)

The titanate nanotubes and nanowires were annealed at 400-600 °C for 1 h. The effect of annealing temperature on the phase transformation and structure of titanate was investigated. From the XRD patterns, the as-prepared material showed poor crystalline quality. This crystalline structure of sample was improved by thermal treatment. Annealing titanate nanotubes at 400 °C resulted in small anatase peaks as displayed in Figure 5.3. When the sample was annealed at 500 °C and 600 °C, the peak intensities corresponding to anatase TiO_2 increased and the sharp peak can be observed due to the crystallinity of anatase TiO_2 increased. In other words, the titanate nanotubes were completely transformed to anatase TiO_2. The results were similar to those reported by others [10, 18].

For the titanate nanowires, after annealed at the temperature in the range of 400-600 °C, a metastable form of titanium dioxide was observed as shown in Figure 5.4. It is suggested that the titanate nanowires were completely dehydrated and re-crystallized into metastable TiO_2 (TiO_2-B) [37, 38]. Further increase annealing temperature to 700 °C, the XRD pattern of anatase TiO_2 was observed (the result not shown). This indicates that metastable TiO_2 (TiO_2-B) was transformed to anatase TiO_2 at this temperature.

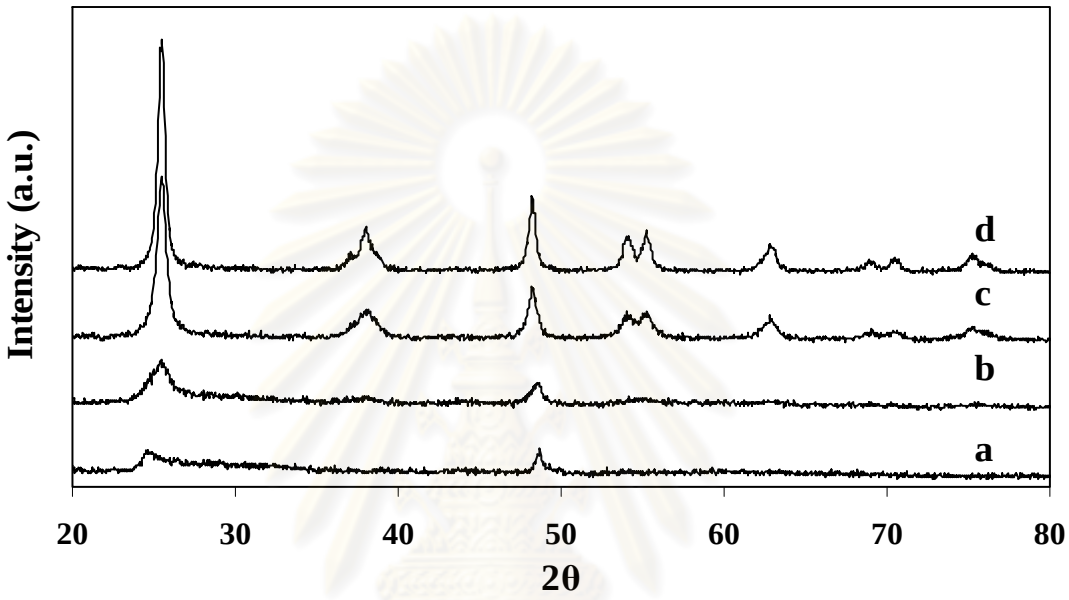

Figure 5.3 XRD patterns of titanate nanotubes: as-synthesized (a), and annealed at 400 °C (b), 500 °C (c), and 600 °C (d)

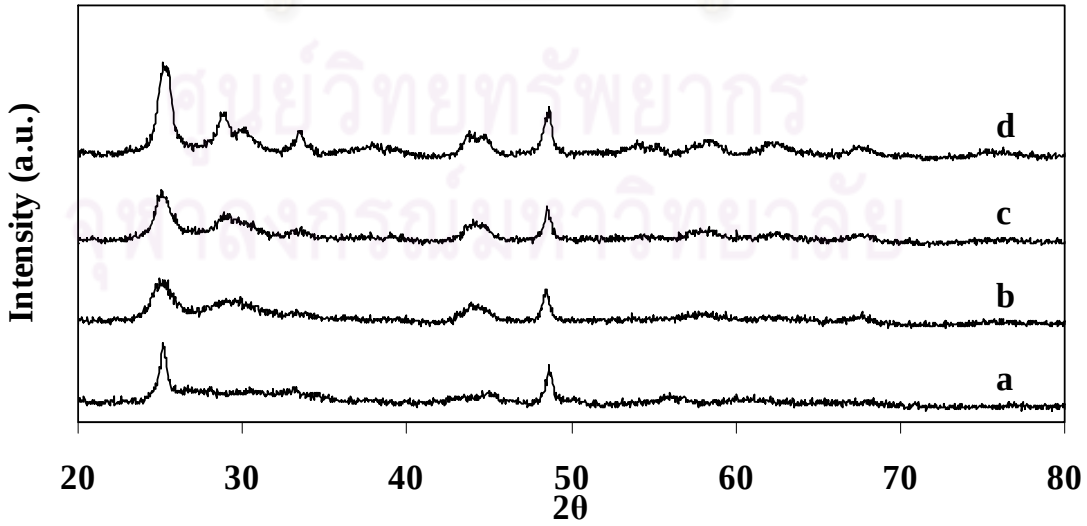

Figure 5.4 XRD patterns of titanate nanowires: as-synthesized (a), and annealed at 400 °C (b), 500 °C (c), and 600 °C (d)

5.1.1.2 Scanning Electron Microscopy (SEM)

Figure 5.5 shows the SEM images of the anatase TiO_2 and samples from hydrothermal process at different reaction temperatures. The different textural characteristics of the products obtained through hydrothermal treatment at various reaction temperatures is shown in Figure 5.5. As can be seen in Figure 5.5 (a) the particles of starting material are spherical. After hydrothermal treatment at 110°C mixed morphologies of nanosheet and nanotubes were observed. At 150 °C the sheet-like structure was completely transformed to tube structure due to additional thermal energy with increasing temperature sufficiently to curl-up the nanosheet into tubular structure due to high surface energy [10]. Titanate nanotubes with diameter ~10-15 nm were synthesized at this temperature. An increase of reaction temperature to 200 °C resulted in the transformation of titanate nanotubes to titanate nanowires as displayed in Figure 5.5 (d). This indicates that temperature of hydrothermal treatment has a strong effect in determining the titanate morphology.

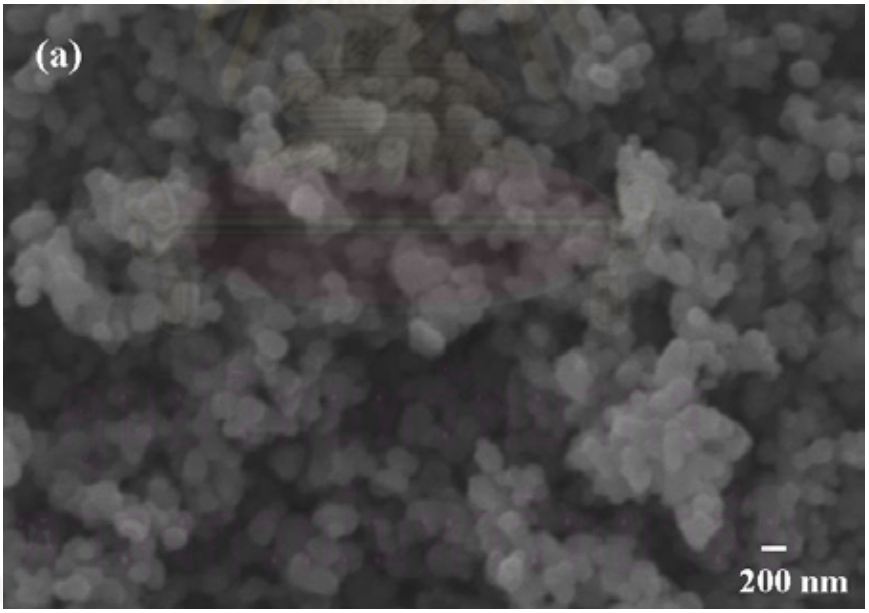

(a) TiO_2 commercial

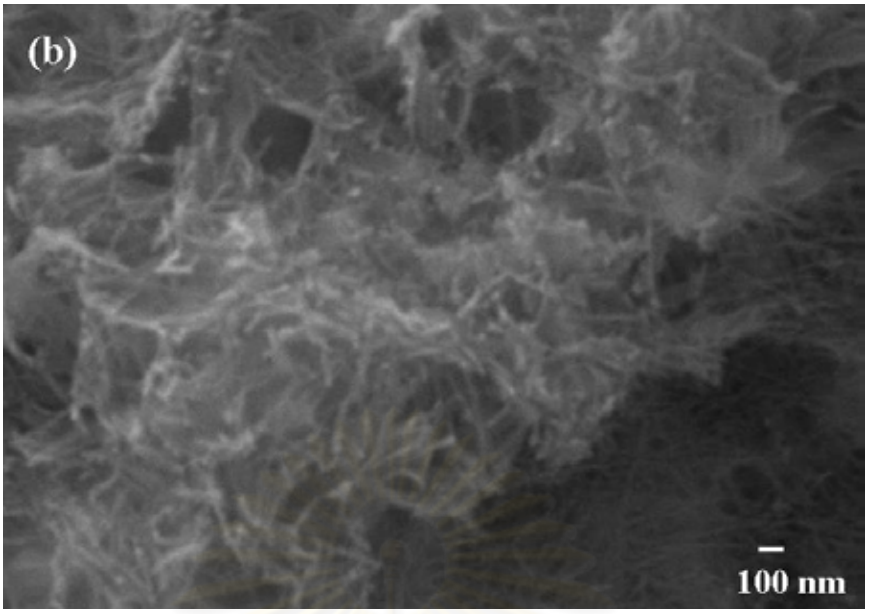

(b) hydrothermal synthesized at 110 °C

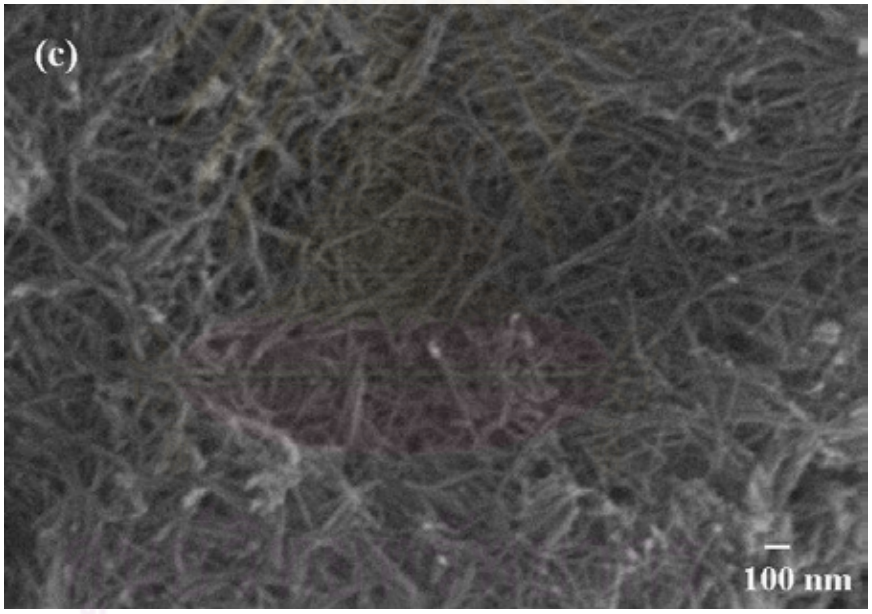

(c) hydrothermal synthesized at 150 °C

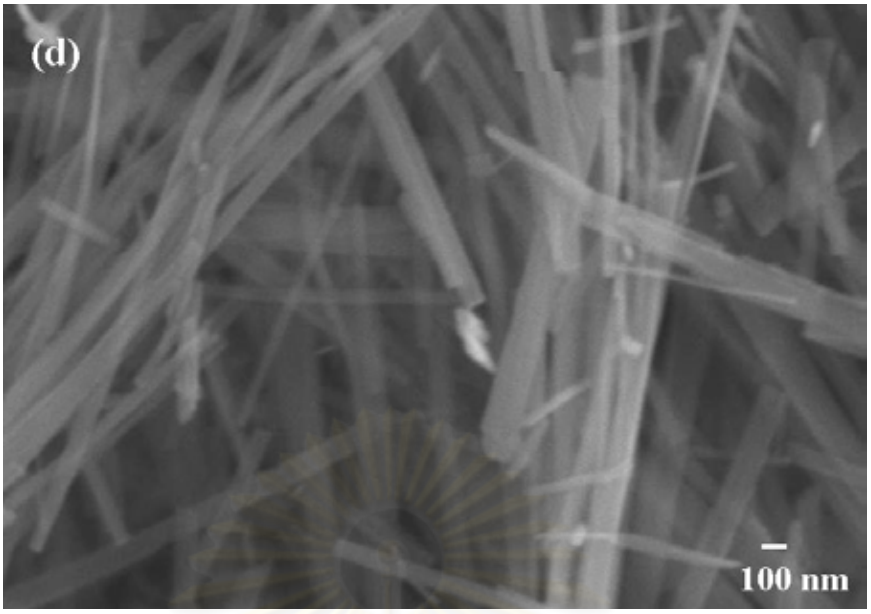

(d) hydrothermal synthesized at 200 °C

Figure 5.5 SEM images of TiO_2 commercial and hydrothermal synthesized materials at various reaction temperatures

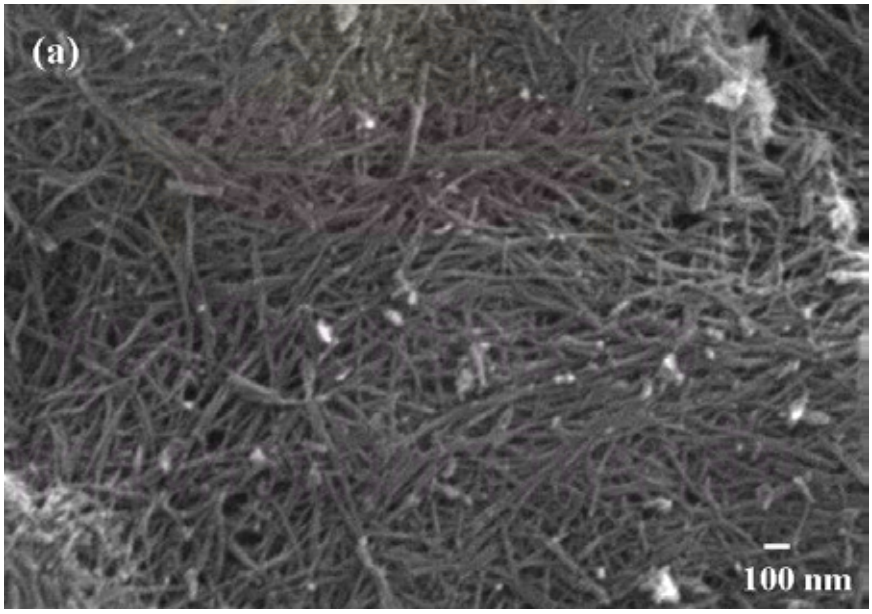

(a) titanate nanotubes synthesized at 150 °C with quenching in ice bath

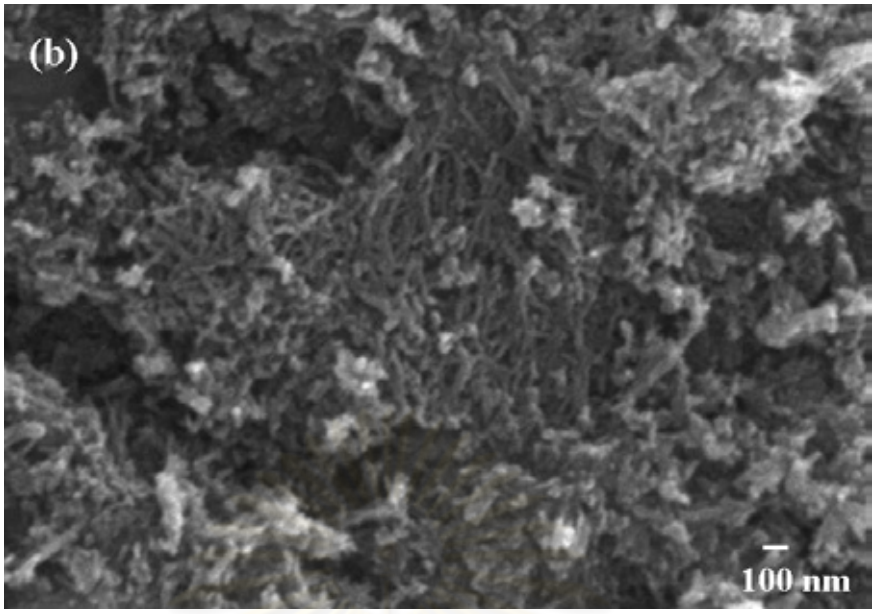

(b) titanate nanotubes synthesized at 150 °C annealed at 600 °C

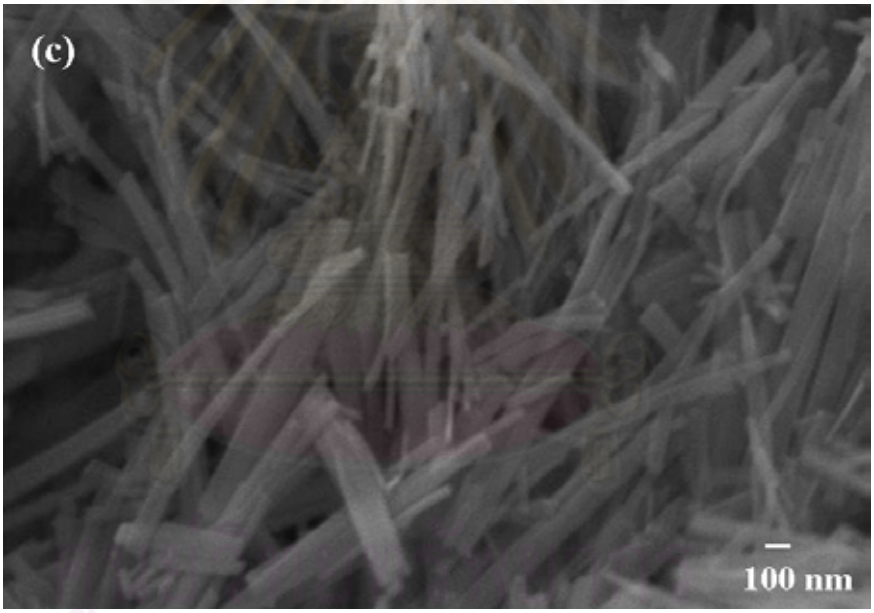

(c) titanate nanowires annealed at 600 °C

Figure 5.6 SEM images of titanate nanotubes synthesized at 150 °C with quenching in ice bath, annealed at 600 °C, and titanate nanowires annealed at 600 °C

The effect of hydrothermal termination procedure was investigated by comparing the products obtained by quenching in an ice bath to those which were naturally cooled down after hydrothermal synthesis at 150 °C. It was found that quenching in an ice bath led to more uniform nanotubes and increased BET surface

area to 210.9 m^2/g. The SEM image of the quenched sample is displayed in Figure 5.6 a.

The SEM images of the samples annealed at 600 °C are shown in Figure 5.6. It can be seen that the tubes were shorter than the as-synthesized materials and some of them were converted to particles due to tubular structure collapsed when annealed at high temperature [6, 10]. For the titanate nanowires, annealing at temperature 600 °C caused only a small decrease in BET surface area but did not affect the morphology as shown in Figure 5.6 c.

5.1.1.3 Transmission Electron Microscopy (TEM)

In order to determine the particle morphology, a powerful technique such as TEM was applied. The TEM micrographs of TiO_2 commercial and samples prepared at different reaction temperatures are shown in Figure 5.7. The morphology of TiO_2 commercial are spherical with diameter > 100 nm. Hydrothermal treatment at 110 °C, some tubes like structure are observed. As seen in Figure 5.7 c, the clearly tubular structure was obtained at 150 °C. The tubular materials were several hundreds of nanometers which outer and inner diameter of nanotubes were approximately 10-12 nm and 4-6 nm, respectively. Increasing temperature to 200 °C led to a transformation of nanotubes to nanowire with non-hollow morphology with a length of several micrometers and width variations between 60-100 nm as shown in Figure 5.7 d. This result corresponds with SEM images.

Zhang *et al.* [39] proposed the formation mechanism of Ti–O nanotubes and nanowires. The formation process for Ti–O nanostructures is simply described as follows. First, the three-dimensional of raw anatase-phase TiO_2, reacts with the NaOH aqueous solution and forms a lamellar product. The lamellar titanate product possesses a two-dimensional layered structure. The nanoscale tubular structure is then achieved by further rolling and one-dimensional nanotubes are formed. The driving force for the scrolling of the nanosheets into nanotubes is proposed to be either the asymmetrical chemical environment on the two opposite sides of the nanosheet or the internal stress arising in multilayered nanosheets from an imbalance in width occurring during crystallization.

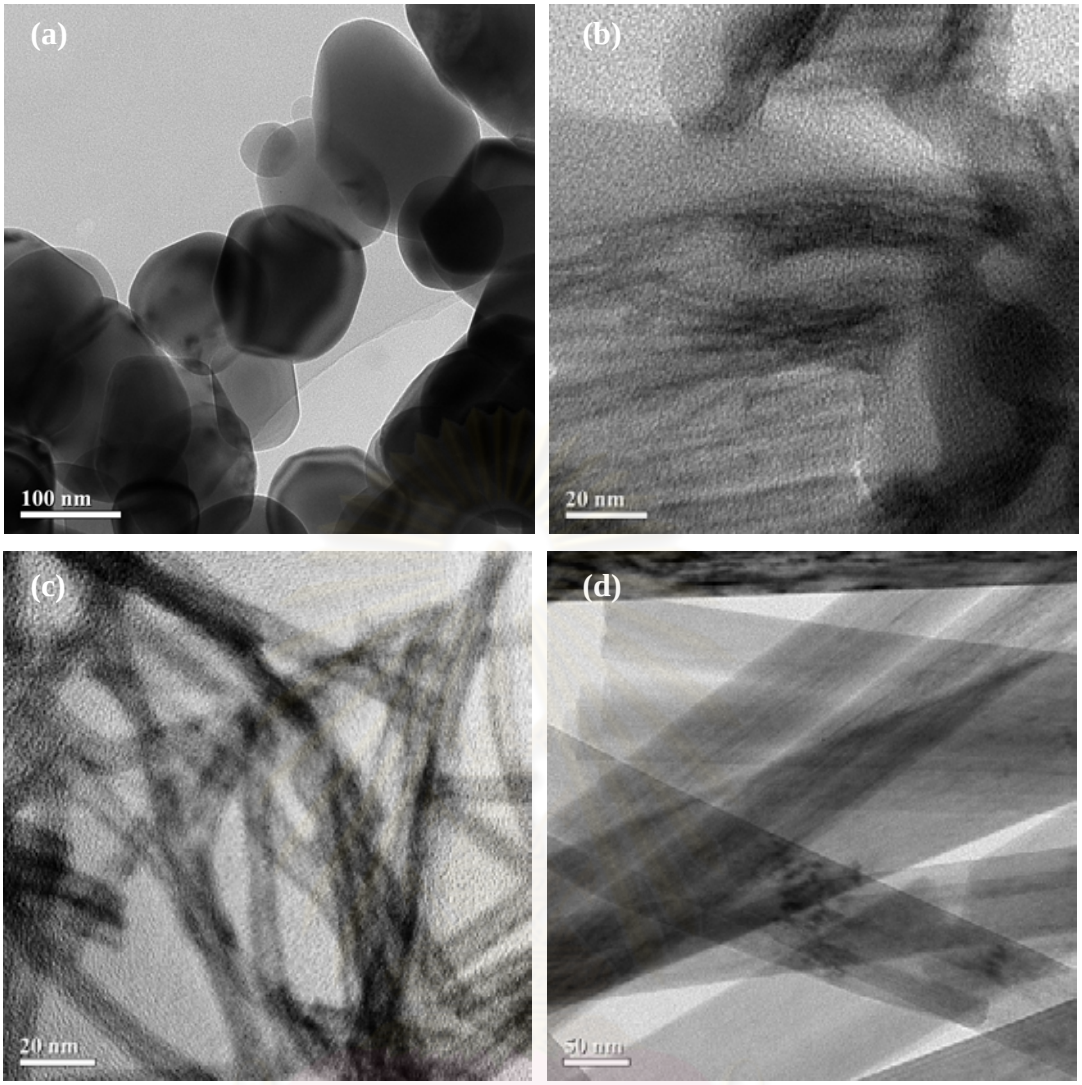

Figure 5.7 TEM images of TiO_2 commercial (a) and hydrothermal synthesized materials at various reaction temperatures: 110 °C (b), 150 °C (c), and 200 °C (d)

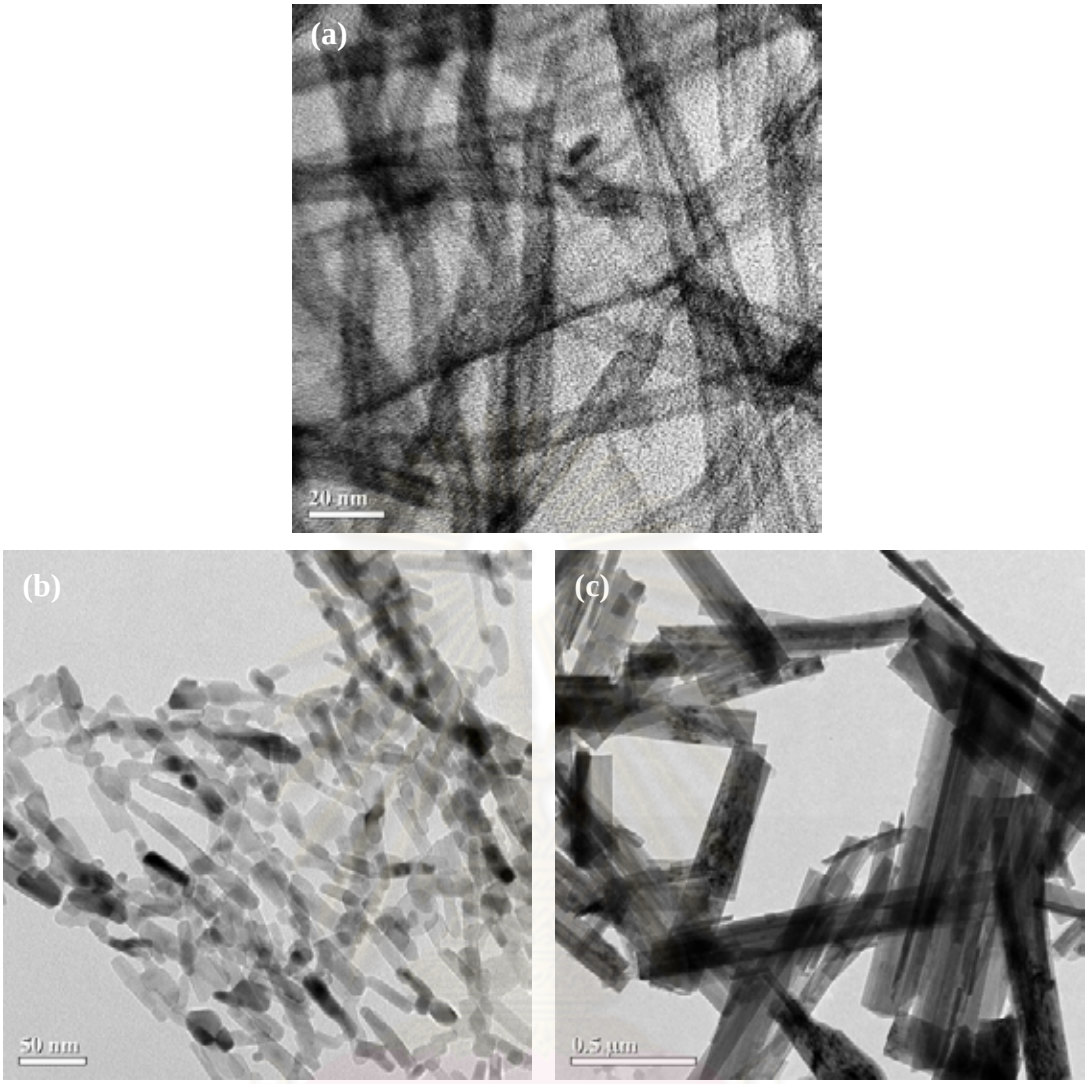

Figure 5.8 TEM images of titanate nanotubes synthesized at 150 °C with quenching in ice bath (a), annealed at 600 °C (b), and titanate nanowires annealed at 600°C (c)

The TEM images of quenched and annealed material are shown in Figure 5.8. The nanotubes structures were clearly observed in the quenched materials after hydrothermal treatment at 150 °C. After thermal treatment at 600 °C, the nanotubes were partially broken and the hollow disappeared, as clearly seen in Figure 5.8 b. The rod-like and some of particles structure were observed. This is in agreement previously reported data concerning the conversion of the titanates into the anatase phase by thermal dehydration [40]. This is associated with the collapse of the interlayer spacing between the walls of the nanotube, resulting of anatase phase that confirmed by XRD results. Therefore, it can be concluded that during the annealing

treatment at high temperature, the chemical bond such as H_2O and –OH are removed from the titanate nanotubes and finally it converts back to the particles again. For titanate nanowire, the morphology was not significant changed after thermal treatment at 600 °C.

5.1.1.4 N_2 physisorption

Specific surface areas of the samples were determined from the N_2 physisorption data measured at liquid nitrogen temperature using Brunauer-Emmett-Teller (BET) technique. Table 5.1 shows the BET surface area of samples obtained at various hydrothermal conditions. The BET surface area of TiO_2 commercial as starting material was 4.8 m^2/g. After hydrothermal treatment at 110 °C resulted in increasing of BET surface area to 157.5 m^2/g. Further increasing hydrothermal temperature to 150 °C, the BET surface area increased to 192.0 m^2/g. Increasing of BET surface areas due to the transformation of morphology from nanosheet to nanotubes which hollow structure that possessed high surface area. The sample synthesized at 200 °C resulted in a low BET surface area (23.2 m^2/g) due to non-hollow structure of titanate nanowire.

For quenching materials, it was found that not only the uniform of tubular structure increased, but the BET surface area of nanotubes also increased. Annealing titanate nanotubes at 600 °C resulted in the decreasing of BET surface area due to the tubes were collapsed and transformed to nanorods and particles shape. This decreasing of surface area corresponds with TEM and SEM results. For the titanate nanowire, annealing at this temperature the BET surface area was not different from the as-synthesized samples.

Table 5.1 BET surface area of titania and titanate support

Hydrothermal temperature	BET surface area (m^2/g)
TiO_2 commercial	4.8
110 °C	157.5
150 °C	192.0
150 °C quenched	210.9
200 °C	23.2
150 °C annealed 600 °C	63.0
200 °C annealed 600 °C	19.4

5.1.2 Characterizations of the supported Pd catalysts

In this section, the titania and titanate supported palladium catalysts were characterized by means of XRD, SEM, TEM, N_2 physisorption in order to investigate the structure and morphology after Pd loading. CO-chemisorption, and ICP were employed to determine the amount of active Pd surface and the actual amount of Pd loading, respectively. The composition of elements on surface and electronic state were analyzed by XPS. To accommodate for discussion, the catalysts used in this research were symbolically assigned as shown in Table 5.2.

Table 5.2 The symbol of the catalysts prepared using the different methods

Catalysts	Symbols
Pd colloid nanoparticles supported on TiO_2 commercial	Pd/TiO_2 com
Pd colloid nanoparticles supported on titanate nanotubes	Pd/TNT
Pd colloid nanoparticles supported on titanate nanowire	Pd/TNW
Pd colloid nanoparticles supported on titanate nanotubes annealed 600 °C	Pd/TNT_600
Pd colloid nanoparticles supported on titanate nanotubes by sonication	Pd/TNT_soni
Pd impregnated on titanate nanotubes by stirring	Imp_stir
Pd impregnated on titanate nanotubes by sonication	Imp_soni

5.1.2.1 X-Ray Diffraction (XRD)

The XRD was performed in order to investigate phase of the Pd supported catalyst. Figure 5.9-5.11 displays XRD patterns of the catalysts prepared from Pd nanoparticles supported on titania and titanate and the catalysts prepared from Pd chloride solution using wet impregnation method. For the Pd^0 metal shows the diffraction peak at 40.1 [3, 33]. All of the catalysts, the diffraction peak of Pd^0 or PdO were not observed. It suggests that palladium was highly dispersed on the titanate surface and/or due to the low amount of Pd loaded on the supports [41]. The XRD patterns of titania and titanate supported Pd nanoparticles catalysts were not significantly different from as-synthesized support. On the other hand, impregnation of Pd chloride on titanate nanotubes support induced disappearance of titanate peak and exhibited the rutile phase of TiO_2, which was confirmed by XRD patterns in Figure 5.11. The diffraction peaks at 27.6 (major), 36.3, 41.5, 44.3, 55.5, 56.9, 63.3, 64.6, and 69.4º can be seen in XRD patterns which corresponding to rutile phase of TiO_2 [37, 42-44]. The phase transformation was probably due to the presence of acid precursor of palladium chloride and calcination at high temperature. According to the literatures, N. Murakami *et al*. [24] reported the transformation of titanate nanotubes to rutile TiO_2 in the presence of Cl^- during hydrothermal. In addition, H.Y. Zhu *et al*.

[45] reported the transformation of titanate nanotubes to rutile TiO_2 in the acidic environment at 60 °C (2.65 M of HNO_3) while other literatures reported that transformation occurred when titanate nanotubes were annealed at above 900 °C [7, 37, 46].

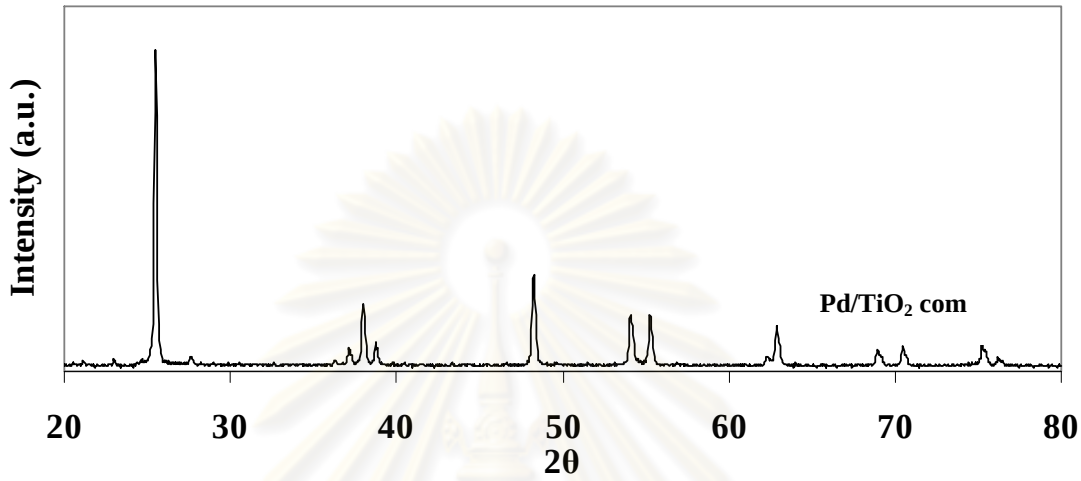

Figure 5.9 XRD pattern of Pd/TiO_2 com

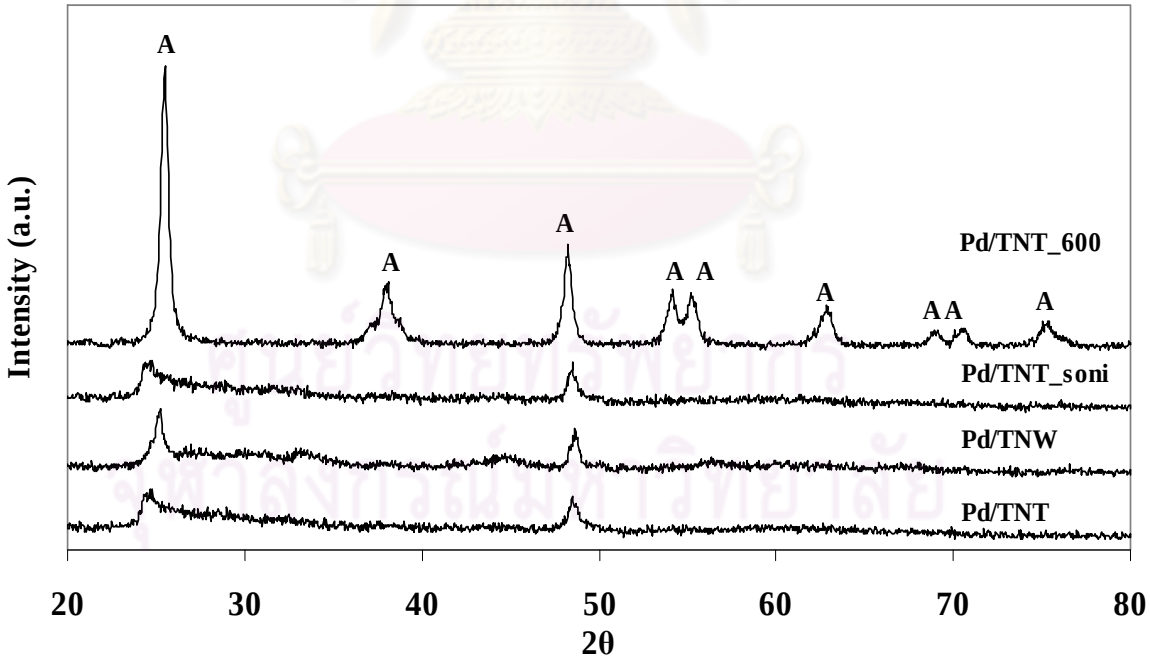

Figure 5.10 XRD patterns of Pd nanoparticles supported on titania and titanate catalysts (A = anatase)

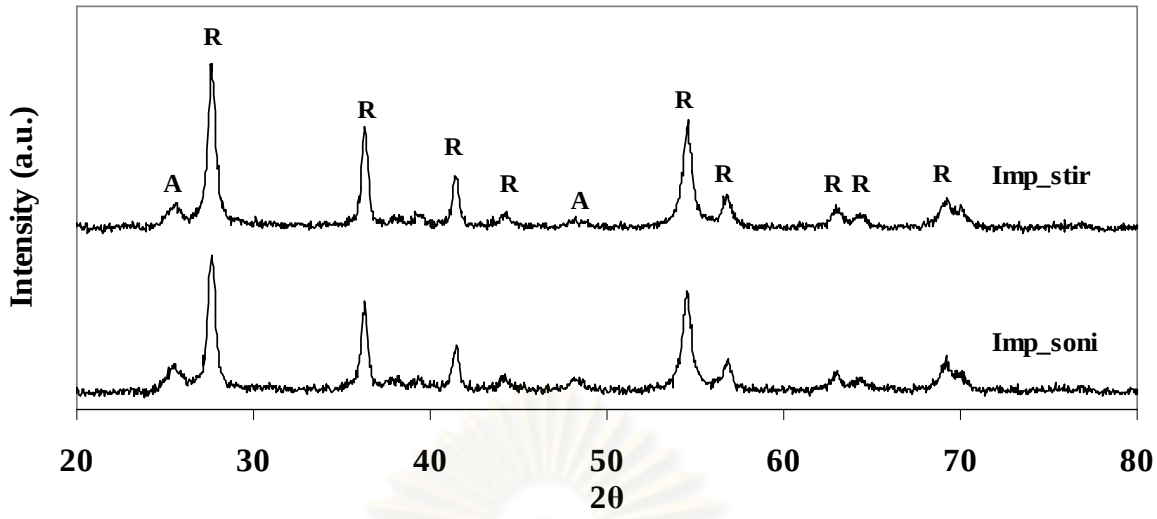

Figure 5.11 XRD patterns of impregnation-made catalysts (A = anatase, R = rutile)

5.1.2.2 Scanning Electron Microscopy (SEM)

The morphologies of supports after Pd loading are shown in Figure 5.12. For Pd nanoparticles catalyst (Figure 5.12 a-e), the morphology of catalysts are not significantly different from as-synthesized. For Pd/TNW catalyst, the titanate nanowires were shorter than before Pd loading. The nanowires may be partially destroyed under stirring in Pd nanoparticles during loading step. The aggregated of rod-like and particles shape were clearly observed in impregnated catalysts (Figure 5.12 f-g). The rod materials were a few hundreds of nanometers which diameter approximately 70-80 nm. The transformation of titanate nanotubes to rod shape occurred during calcination step in the acidic environment, which was confirmed by XRD result.

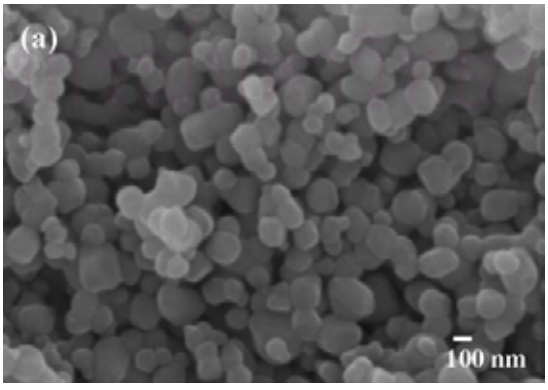

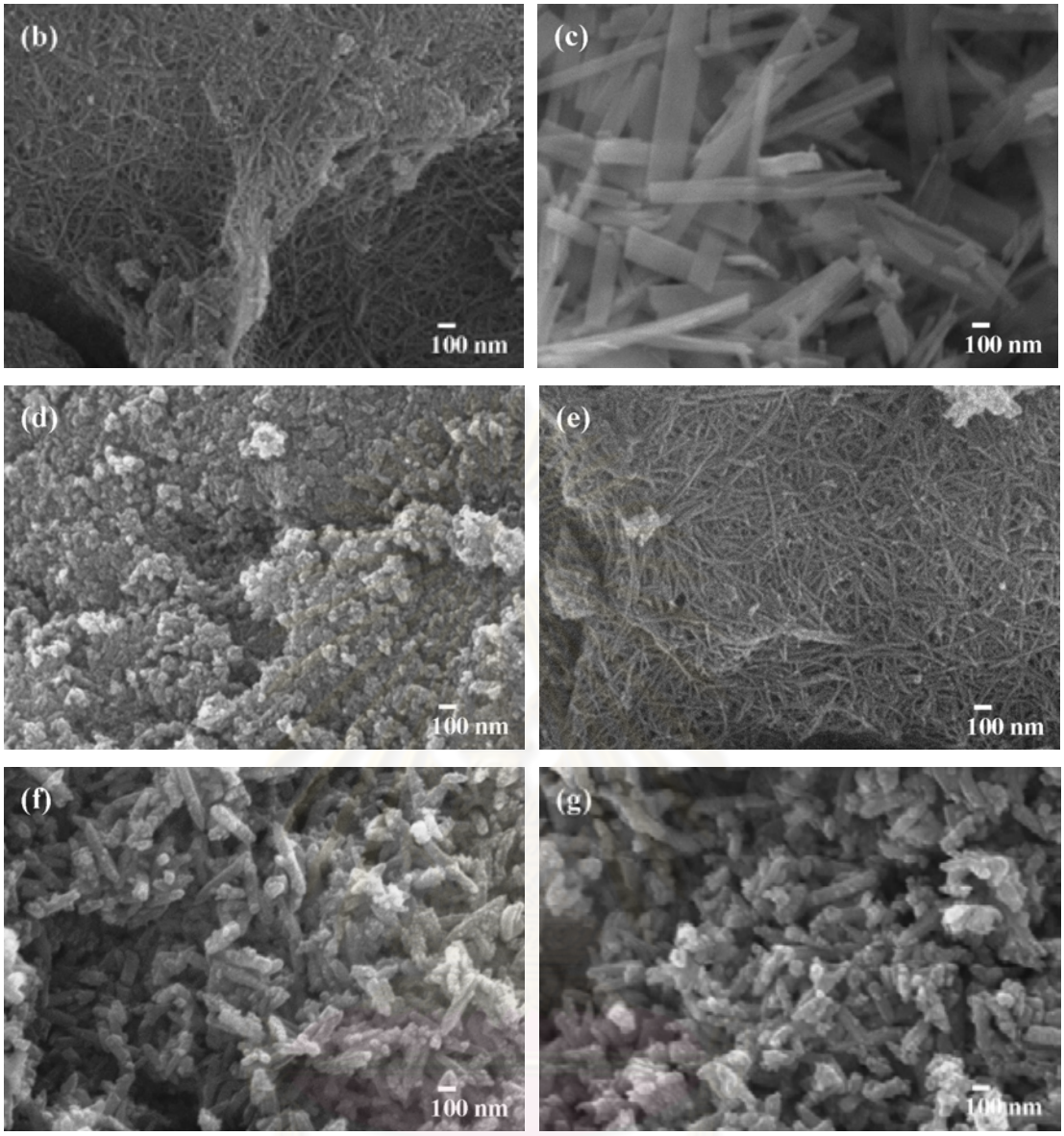

Figure 5.12 SEM images of catalysts: Pd/TiO_2 com (a), Pd/TNT (b), Pd/TNW (c), Pd/TNT_600 (d), Pd/TNT_soni (e), Imp_stir (f), and Imp_soni (g)

5.1.2.3 Transmission Electron Microscopy (TEM)

The morphology of catalysts was observed by transmission electron microscopy (TEM). The TEM images of all catalysts after Pd loading are displayed in Figures 5.13. The Pd nanoparticles prepared via reduction by solvent method were loaded on various supports as displayed in Figure 5.13 a-e. It appears that the particle size and shape of the catalysts were not affected by loading of palladium (no changes in the particle size and shape). The small dark spots in catalyst represented the Pd

particles. In the case of Pd nanoparticles supported on titania and titanate, no Pd cluster was observed in TEM images (clearly seen in Pd/TNW). The average particles sizes of Pd were about 4-5 nm. The larger Pd particle sizes were observed on catalysts prepared by impregnation method in Figure 5.13 f and g. In addition, morphologies of the catalysts were changed after impregnation step. The presence of acid precursor of palladium chloride and calcination at high temperature results in the collapse of nanotubes. The large rods and non-hollow structures were observed. This TEM images corresponds with the SEM results.

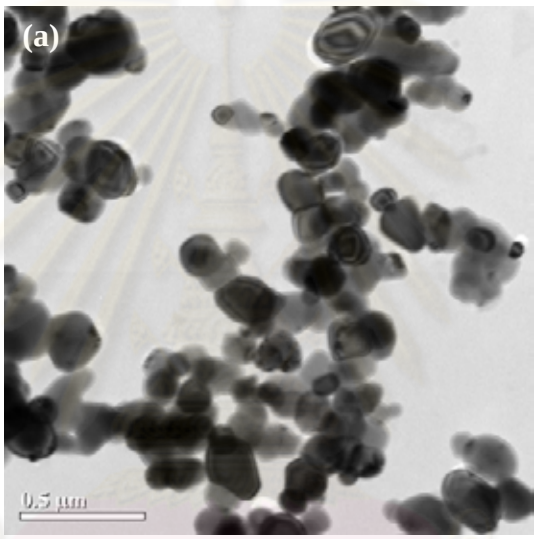

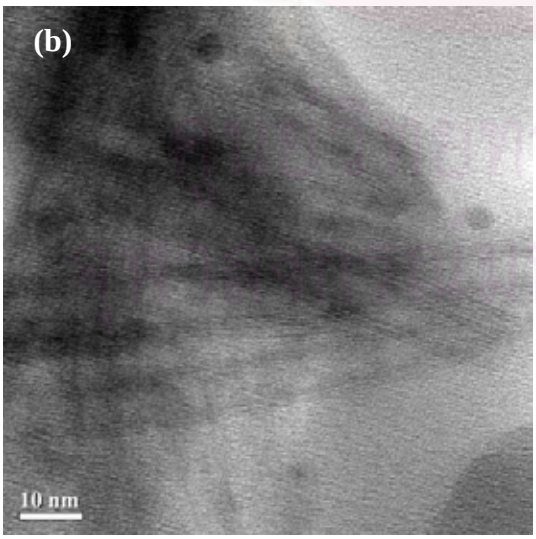

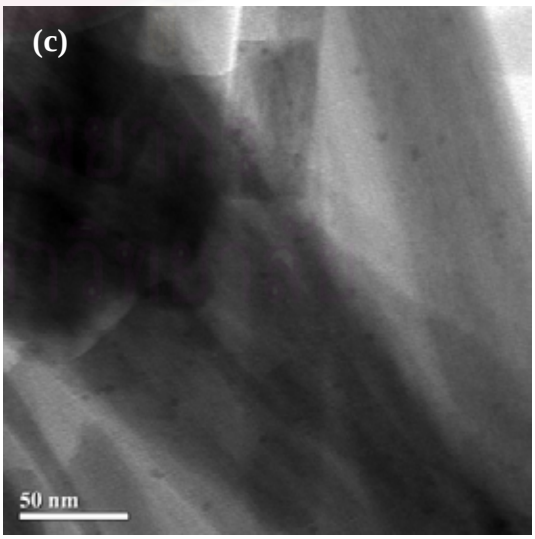

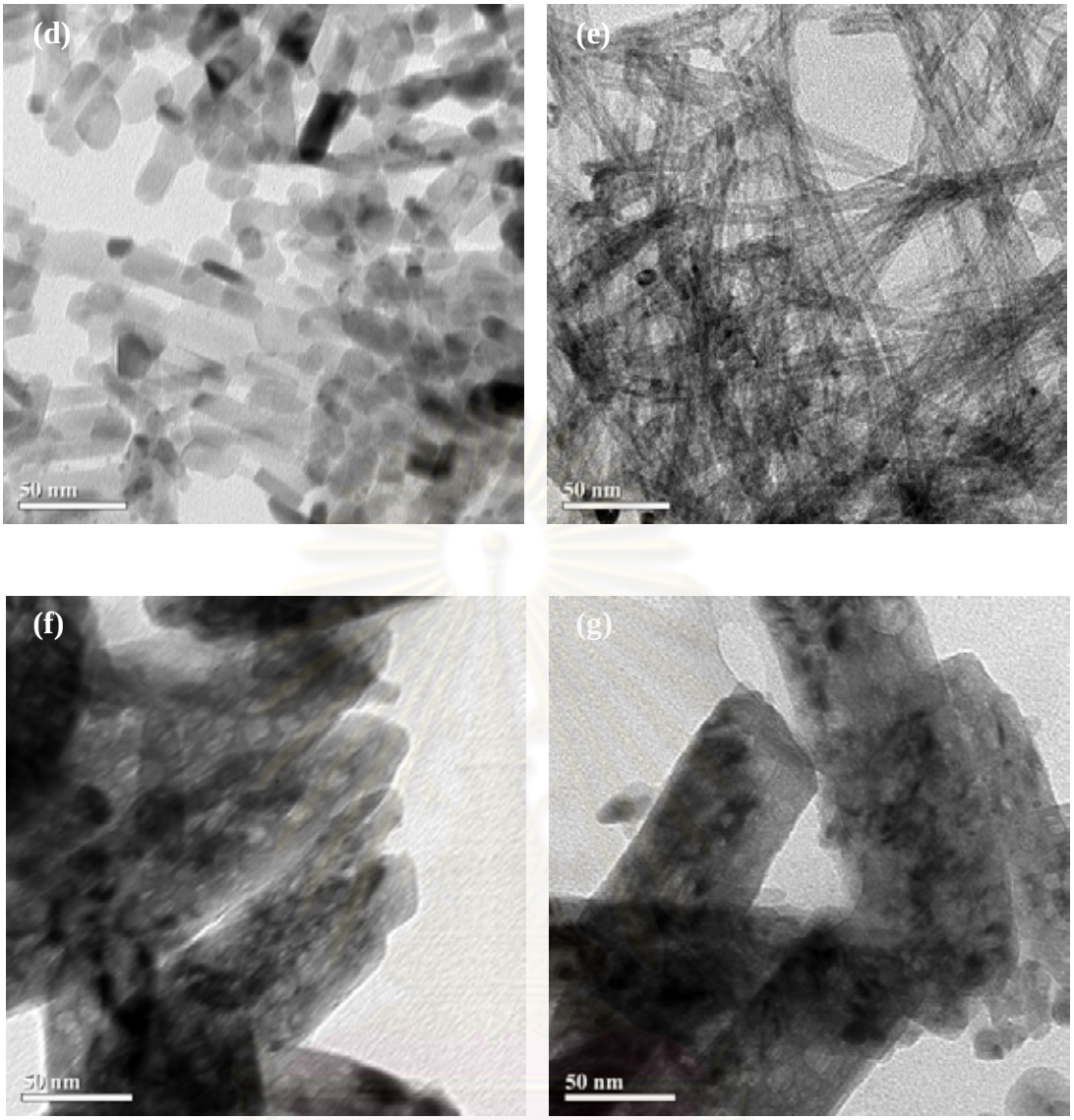

Figure 5.13 TEM images of catalysts: Pd/TiO_2 com (a), Pd/TNT (b), Pd/TNW (c), Pd/TNT_600 (d), Pd/TNT_soni (e), Imp_stir (f), and Imp_soni (g)

5.1.2.4 N_2 physisorption

The BET surface area of Pd based catalysts was determined by adsorption and condensation of N_2 at liquid N_2 temperature (-196 °C). The results of BET surface area are given in Table 5.3. The Pd nanoparticles loaded on titania and titanate supports slightly decreased the BET surface area of the catalysts. This was suggested that Pd were deposited in the pores of supports, similar to those reported in the literatures [1, 47]. The impregnation catalysts possessed low BET surface area due to the transformation of titanate nanotubes to larger rutile TiO_2 during calcination step, as

confirmed by XRD results. The rutile TiO_2 exhibited the rod-like shape that can be clearly observed from SEM images.

Table 5.3 BET surface area of catalysts

Catalysts	BET surface area (m^2/g)
Pd/TiO_2 com	4.4
Pd/TNT	185.0
Pd/TNW	19.8
Pd/TNT_600	41.1
Pd/TNT_soni	190.7
Imp_stir	20.3
Imp_soni	22.1

5.1.2.5 X-ray Photoelectron Spectroscopy (XPS)

XPS was performed to determine the composition of element on catalyst surface and electronic state. The XPS results such as binding energies and surface composition of catalysts are shown in Figure 5.14. The analysis results from XPS are also reported in Table 5.3 and 5.4. No distinctive peaks for Pd $3d_{5/2}$ were observed Pd nanoparticles loaded on support, indicating very low amount of Pd present on the catalyst surface. It was found that Pd nanoparticles loading by sonication (Pd/TNT_soni) led to the appearance of binding energies of Pd $3d_{5/2}$ at 335.1 eV corresponding to Pd^0 [1, 3] It was suggested that sonication increased Pd surface concentration. The impregnation-made catalyst appeared at 337.4 and 337.6 eV indicating the PdO corresponding to calcined sample.

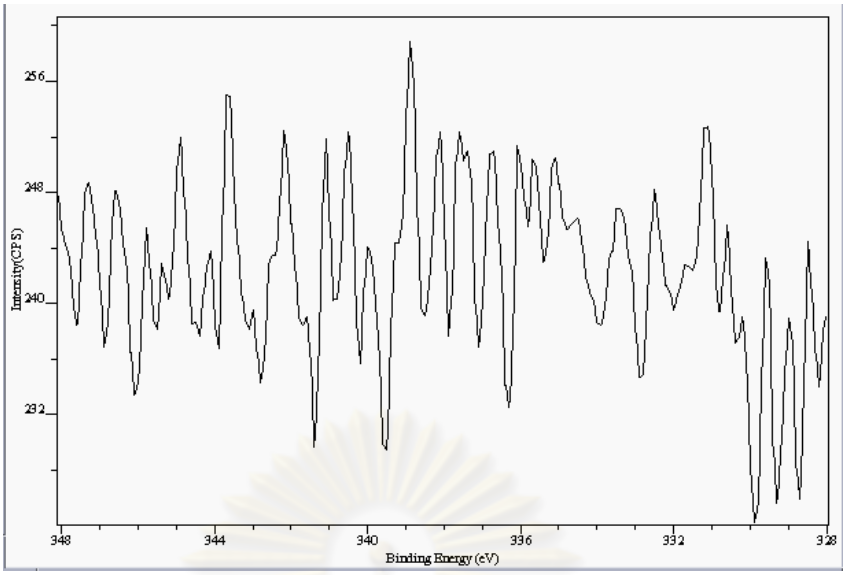

(a) Pd/TNT

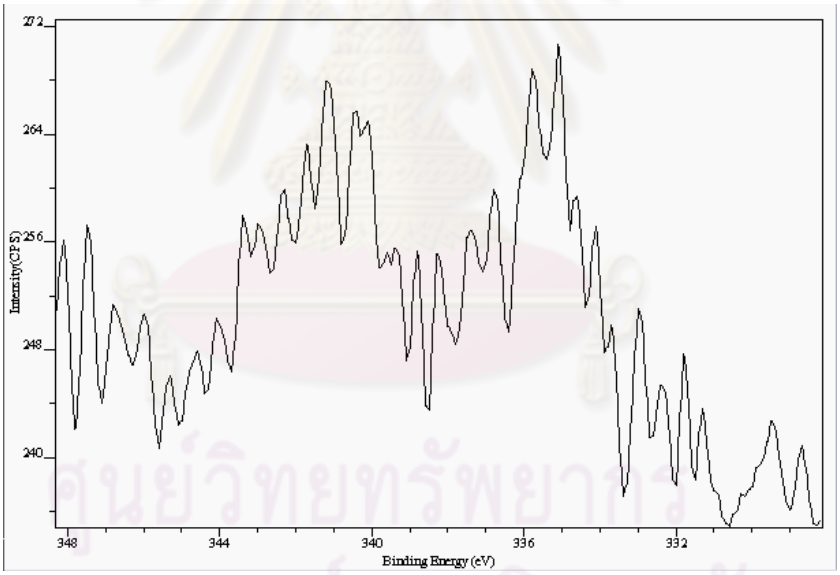

(b) Pd/TNT_soni

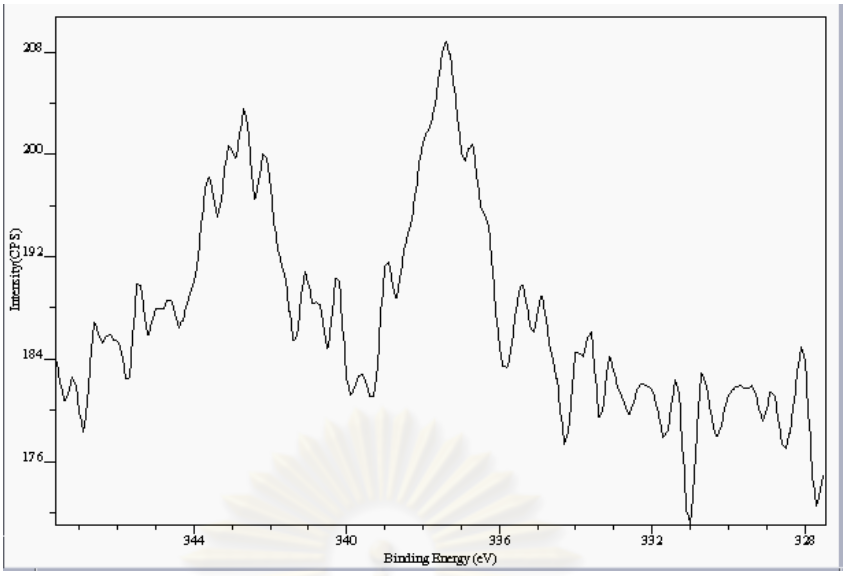

(c) Imp_soni

Figure 5.14 XPS results of catalysts

Table 5.4 XPS results of all catalysts

Catalysts	Pd 3d		Ti 2p	
	B.E. (ev)	**FWHM**	**B.E. (ev)**	**FWHM**
Pd/TiO_2 com	n.d.*	-	458.9	1.303
Pd/TNT	n.d.	-	458.8	1.497
Pd/TNW	n.d.	-	458.9	1.915
Pd/TNT_600	n.d.	-	458.8	1.346
Pd/TNT_soni	335.1	1.410	458.5	1.571
Imp_stir	337.6	1.316	458.9	1.618
Imp_soni	337.4	1.787	458.6	1.555

* n.d. = not determined

The percentages of atomic concentration and Pd/Ti ratio are also given in Table 5.5. The Pd/TNT_soni catalysts showed higher Pd/Ti ratio indicating that concentration of Pd at surface increased when sonication treatment. It is in good agreement with the active site from CO chemisorption results.

Table 5.5 Atomic concentration from XPS results

Catalysts	Atomic conc. (%)		Pd/Ti
	Pd 3d	Ti 2p	
Pd/TiO_2 com	n.d.	10.12	n.d.
Pd/TNT	n.d.	11.28	n.d.
Pd/TNW	n.d.	10.01	n.d.
Pd/TNT_600	n.d.	13.51	n.d.
Pd/TNT_soni	0.09	10.69	0.0084
Imp_stir	0.16	11.62	0.0138
Imp_soni	0.20	9.67	0.0207

5.1.2.6 Inductive Coupled Plasma Optical Emission Spectrometer (ICP-OES)

The actual amount of Pd loading was confirmed by inductive coupled plasma optical emission spectrometer (ICP-OES). All the catatysts, 1 wt% of Pd was loaded on support. For Pd colloid nanoparticles loading, it can be observed that the initially targeted 1wt% Pd loading was not really achieved. Therefore, the rest of the metal was lost during the synthesis procedure, probably during the washing step. For Pd/TiO_2 com, the actual content of Pd was very low about 0.02 wt% of catalyst. The low amount of Pd may due to low surface area of commercial TiO_2 support. Others catalysts possess the palladium contents in the range of 0.48-0.57 wt%. For impregnation-made catalyst, the palladium concentrations were 1.01 and 1.27 wt% for Imp_stir and Imp_soni catalyst, respectively. It was seen that sonication can slightly enhanced the palladium contents for both of Pd nanoparticles loading and impregnation catalysts.

Table 5.6 Actual amount of Pd loading measured by ICP

Catalysts	Actual amount of Pd (wt%)
Pd/TiO_2 com	0.02
Pd/TNT	0.51
Pd/TNW	0.48
Pd/TNT_600	0.56
Pd/TNT_soni	0.57
Imp_stir	1.01
Imp_soni	1.27

5.1.2.7 CO-Pulse Chemisorption

The relative amounts of active surface Pd metals on the catalyst samples were calculated from CO chemisorption experiments at room temperature. The calculation based on the assumption that one carbon monoxide molecule adsorbs on one palladium site [48]. The amounts of CO chemisorption on the catalysts, the percentages of Pd dispersion, and the average Pd metal particle sizes calculated based on the CO chemisorption results are given in Table 5.7. The active sites of catalysts varied from 0.51-11.21 $\times$ 10^{18} site/g_{cat}. Among these catalysts, Pd/TiO_2 com exhibited the lowest Pd active sites. The highest Pd active site and dispersion was found in Pd/TNT_soni. The high surface area of titanate nanotubes promoted dispersion of Pd metal [49, 50]. It was suggested that sonication enhanced the palladium deposition which was consistent with XPS and ICP results. It is indicated that smaller Pd nanoparticles, higher dispersion, and higher Pd surface area were prepared from reduction by solvent method. The corresponding Pd^0 particle sizes calculated based on CO chemisorption were varied from 3.1-11.1 nm.

Table 5.7 The results obtained from CO chemisorption

Catalysts	Active site[a] ($\times 10^{-18}$ site/g_{cat})	Pd dispersion[b] (%)	metallic surface area (m^2/g of Pd)	Particle size (nm)
Pd/TiO_2 com	0.51	n.d.[c]	n.d.	n.d.
Pd/TNT	9.13	31.7	141	3.5
Pd/TNW	7.09	26.1	116	4.3
Pd/TNT_600	6.57	20.8	93	5.4
Pd/TNT_soni	11.21	35.7	159	3.1
Imp_stir	5.82	10.2	45	11.1
Imp_soni	10.40	14.4	64	7.8

[a]Error of measurement = +/- 5 %

[b]Based on the actual amount of Pd loading determined by inductive coupled plasma (ICP)

[c]n.d. = not determined

5.2 Catalytic performance for 1-heptyne hydrogenation

The catalytic performance of catalysts was investigated in the liquid-phase selective hydrogenation of 1-heptyne to 1-heptene. The reaction was carried out in a batch system in a 50 ml stainless-steel autoclave reactor. In this study, 0.02 g of catalyst was reacting with 10 ml of 2 vol.% of 1-heptyne in toluene under mild condition (30 $^{\circ}$C, 1 atm) for 5-40 minutes. The reaction was operated with high stirring rate (1000 rpm) in order to eliminate the external mass transfer of hydrogen problem. The liquid reactants and products were analyzed by gas chromatography equipped with FID detector.

The performance of catalysts was determined in terms of 1-heptyne conversion and selectivity towards heptene. The conversions of 1-heptyne versus reaction time are shown in Figure 5.15. Under similar reaction conditions, the hydrogenation rate of Pd nanoparticles supported titanate catalysts exhibited higher 1-heptyne conversion than the impregnated ones. Among these Pd nanoparticles

catalysts, Pd/TiO_2 com exhibited lowest conversion, according to the lower metal active sites as determined from CO chemisorption. At 5 min reaction time, the conversion of Pd/TNT was 40 %. It was found that sonication clearly increased conversion of 1-heptyne to 55 % that consistent with amount of Pd active sites and highly dispersion from CO chemisorption result. Increasing of conversion due to the sonication may enhance the content of palladium deposits. The XPS result confirmed that Pd at surface increased when sonication was applied. Lucky M. Sikhwivhilu *et al.* [31] reported that the high surface area and porosity of nanotubular catalysts promise to be advantageous for catalytic activity for hydrogenation of phenol to cyclohexanone. For Pd nanoparticles based catalysts, 1-heptyne was completely converted with in 30 min of reaction time, except Pd/TiO_2 com catalyst.

For impregnated catalysts, they exhibited rutile phase of TiO_2 that possess low BET surface area. The presence larger of Pd particles size and low dispersion (calculated from CO chemisorption) results in low catalytic activity of catalyst. The conversion of 1-heptyne increased with increasing reaction time. 1-heptyne was completely converted for 40 min reaction which was slower than those of Pd nanoparticles loading catalysts.

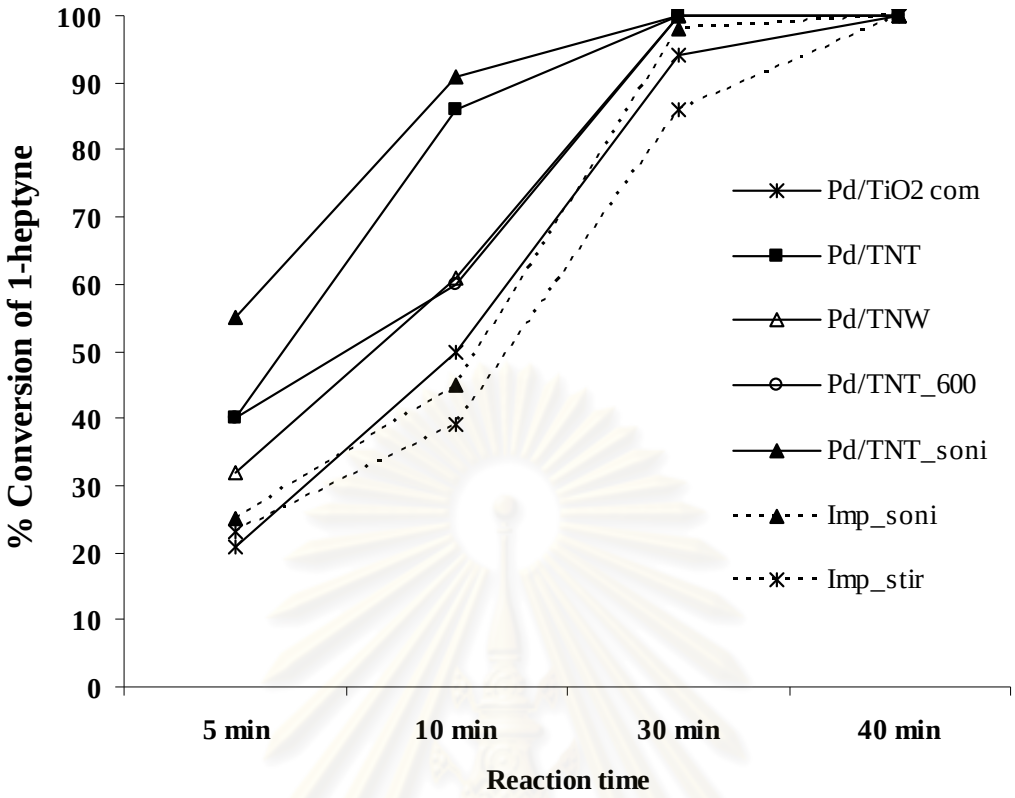

Figure 5.15 Conversion of Pd based catalysts in liquid phase selective hydrogenation of 1-heptyne at various reaction times (30 °C, H_2 pressure 1atm)

The selectivity of 1-heptene obtained over various catalysts is displayed in Figure 5.16. At 5 min reaction time, 1-heptene selectivity of Pd nanoparticles based catalysts was about 92 %. For impregnation catalyst, they showed higher selectivity of 1-heptene (~ 96 %). For 30 min reaction, the selectivity of 1-heptene of Pd nanoparticles supported titanate decreased to ~ 60-65 % and not significantly changed for 40 min reaction. These decreasing of selectivity due to heptene undergo hydrogenation to heptane. At complete conversion (40 min), the Pd/TiO_2 com gave lower selectivity of 1-heptene than those of the other catalysts. The high selectivity (82 %) was observed on Imp_soni catalyst due to sonication enhanced the deposit of palladium contents. It was remarked that the Pd supported on titania and titanate nanotubes derived hydrothermal synthesized catalysts not only increased conversion of 1-heptyne, but also maintained the moderate selectivity of heptene.

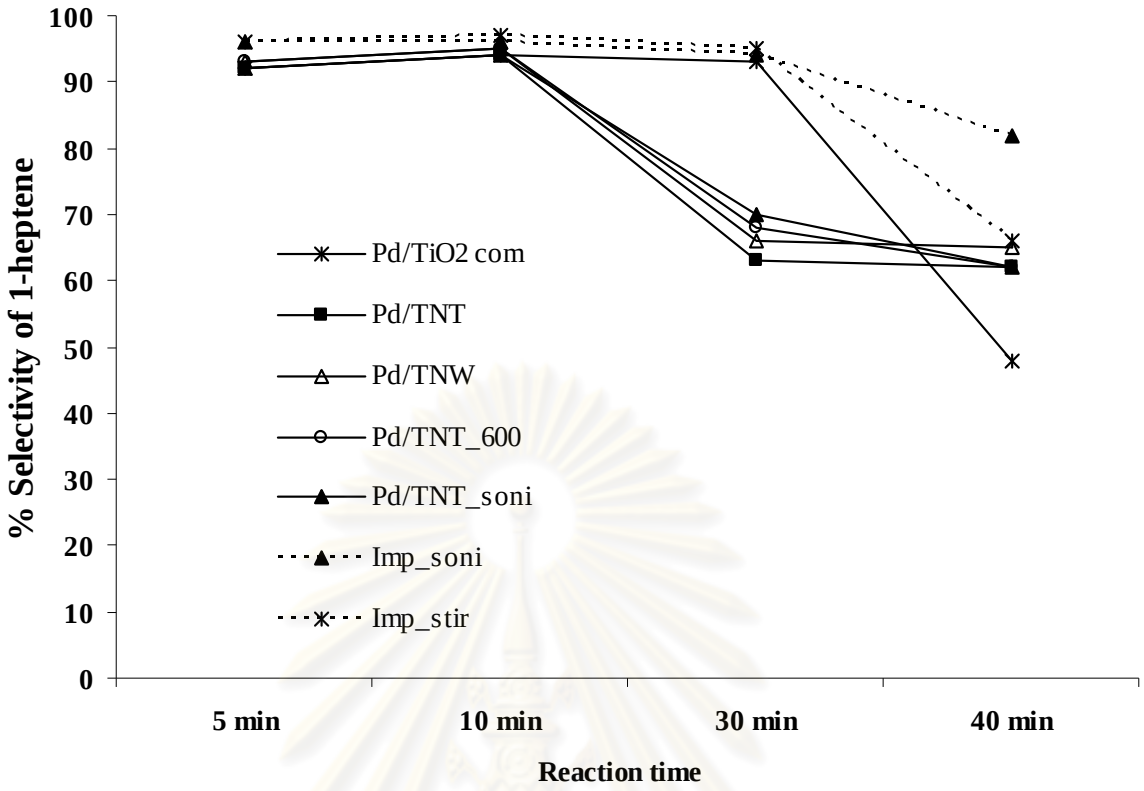

Figure 5.16 Selectivity of Pd based catalysts in liquid phase selective hydrogenation of 1-heptyne at various reaction times (30 °C, H_2 pressure 1atm)

Figure 5.17 shows the yield of heptene of catalysts versus reaction time. For 5-10 min reaction, the Pd nanoparticles supported catalyst showed higher yield than impregnation-made catalyst. The highest yield of heptene was observed in Pd/TNT_soni. Yield of heptene further decreased with increasing reaction time to 30 min, this suggested that heptene undergo hydrogenation to heptane. At complete conversion, all the catalysts exhibited 60-65 % yield of heptene, except Pd/TiO_2 com and Pd/TNT_soni showed 48 % and 82 % yield, respectively.

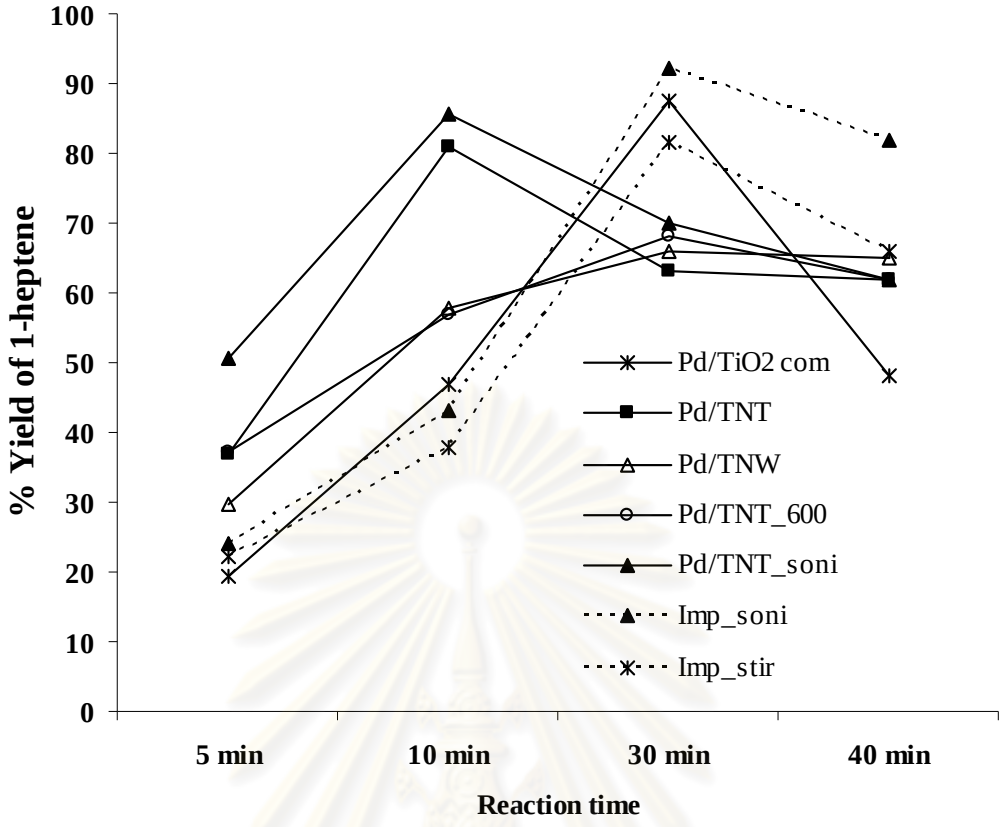

Figure 5.17 Yield of Pd based catalysts in liquid phase selective hydrogenation of 1-heptyne at various reaction times (30 $^{\circ}$C, H_2 pressure 1atm)

The reaction rate and turnover frequencies (TOFs) of catalysts are presented in Table 5.8. Reaction rate of catalysts varied in the range 3.22-8.4$\times 10^{18}$ molecules/g_{cat}s. The Pd/TiO_2 com gave the lowest reaction rate while highest hydrogenation rate was obtained on Pd/TNT_soni catalyst. The impregnation catalyst exhibited lower reaction rate than Pd colloid nanoparticles loading. The reaction rate increased with increasing Pd active sites and Pd dispersion which obtained from CO chemisorption results. The turnover frequencies (TOFs) is defined as mole of product per active site per time which calculated based on CO chemisorption results. From Table 5.8, TOF of catalysts were between 0.37-0.93 s^{-1}.

Table 5.8 Initial reaction results of the catalysts based on 5 min reaction

catalysts	% conversion	% selectivity	Reaction rate ($\times 10^{-18}$molecules/g_{cat} s)	TOF (s^{-1})
Pd/TiO_2 com	21	92	3.22	n.d.*
Pd/TNT	40	92	6.13	0.67
Pd/TNW	32	93	4.91	0.69
Pd/TNT_600	40	93	6.13	0.93
Pd/TNT_soni	55	92	8.44	0.75
Imp_stir	23	96	3.53	0.61
Imp_soni	25	96	3.83	0.37

*n.d. = not determined

CHAPTER VI

CONCLUSIONS AND RECOMMENDATIONS

This chapter is composed of two sections, section 6.1 reveals the conclusions obtained from the experimental results of the prepared catalysts and the catalytic studies in the liquid-phase selective hydrogenation of 1-heptyne to heptene. Additionally, the recommendations for further study are given in section 6.2.

6.1 Conclusions

1. Titanate nanotubes and nanowires were synthesized by using hydrothermal process at various temperatures ranging between 110°C-200 °C. After hydrothermal treatment at 110 °C, the spherical titania particles were transformed into mixed nanosheet and nanotubes structure. At 150 °C, the titanate nanosheets were completely transformed into nanotubes. Further increasing reaction temperature to 200 °C resulted in the transformation of titanate nanotubes into titanate nanowires.

2. Quenching sample in an ice bath after hydrothermal treatment not only increased the uniform morphology, but also increased the BET surface area of titanate nanotubes.

3. Annealing at 600 °C, the titanate nanotubes were transformed back into anatase TiO_2 while annealing titanate nanowires at 600 °C resulted in the transformation of titanate nanowires to metastable TiO_2, instead.

4. The Pd catalysts supported on titanate nanotubes exhibited better performance in the liquid phase selective hydrogenation of 1-heptyne to 1-heptene than the ones supported on titanate nanowire and the commercial titania.

5. Using titanate nanotubes as the catalyst support, the synthesis of Pd nanoparticles from reduction by solvent method exhibited higher conversion than the catalysts prepared by conventional impregnation method. However, at completed

conversion of 1-heptyne, the impregnation-made catalysts showed higher 1-heptene selectivity.

6. The hydrogenation rate increased with increasing Pd dispersion. However, the selectivity to 1-heptene depended largely on nature of TiO_2 support, and/or the interaction of Pd and titania support.

6.2 Recommendations

1. The simultaneous synthesis of Pd nanoparticles synthesized from reduction by solvent method and titania during hydrothermal process should be investigated.

2. The other precursors of Pd should be used for impregnation to prevent the transformation to rutile phase.

REFERENCES

[1] Mekasuwandumrong, O., Somboonthanakij, S., Praserthdam, P., and Panpranot, J. Preparation of nano-Pd/SiO_2 by one-step flame spray pyrolysis and its hydrogenation activities: Comparison to the conventional impregnation method. Industrial & Engineering Chemistry Reseach 48 (2009): 2819-2825.

[2] Sirikajorn, T., Mekasuwandumrong, O., Praserthdam, P., James G. Goodwin, Jr., and Panpranot, J. Effect of support crystallite size on catalytic activity and deactivation of nanocrystalline $ZnAl_2O_4$-supported Pd catalysts in liquid-phase hydrogenation. Catalysis Letters 126 (2008): 313-318.

[3] Somboonthanakij, S. et al. Characteristics and catalytic properties of Pd/SiO_2 synthesized by one-step flame spray pyrolysis in liquid-phase hydrogenation of 1-heptyne. Catalysis Letters 119 (2007): 346-352.

[4] Mekasuwandumrong, O., Phothakwanpracha, S., Jongsomjit, B., Shotipruk, A., and Panpranot, J. Liquid-phase selective hydrogenation of 1-heptyne over Pd/TiO_2 catalyst synthesized by one-step flame spray pyrolysis. Catalysis Letters 136 (2010): 164-170.

[5] Lederhos, C. R., Badano, J. M., Mónica, E., Quiroga e Pablo, and L' Argentière, C. Influence of Ni addition to a low loaded palladium catalyst on the selective hydrogenation of 1-heptyne. Quimica Nova 33 (2010): 816-820.

[6] Cesano, F. et al. Designing TiO_2 based nanostructures by control of surface morphology of pure and silver loaded titanate nanotubes. Journal of Physical Chemistry C 114 (2010): 169-178.

[7] Cho, J. M., Seo, J. M., Lee, J.-K., Zhang, H., and Lamb, R. Electronic properties of oxygen vacancies in titania nanotubes. Physica B 404 (2009): 127-130.

[8] Zhao, Q., Li, M., Chu, J., Jiang, T., and Yin, H. Preparation, characterization of Au (or Pt)-loaded titania nanotubes and their photocatalytic activities for degradation of methyl orange. Applied Surface Science 255 (2009): 3773-3778.

[9] Ou, H. H., and Lo, S. L. Review of titania nanotubes synthesized via the hydrothermal treatment: Fabrication, modification, and application. Separation and Purification Technology 58 (2007): 179-191.

[10] Seo, H. K. et al. A study on the structure/phase transformation of titanate nanotubes synthesized at various hydrothermal temperatures. Solar Energy Materials & Solar Cells 92 (2008): 1533-1539.

[11] Viriya-empikul, N. et al. Effect of preparation variables on morphology and anatase-brookite phase transition in sonication assisted hydrothermal reaction for synthesis of titanate nanostructures Materials Chemistry and Physics 118 (2009): 254–258.

[12] Shunlil, Z. et al. Morphological structure and physicochemical properties of nanotube TiO_2. Chinese Science Bulletin 45 (2000): 1533-1536.

[13] Zhou, W. et al. One-dimensional single-crystalline Ti–O based nanostructures: properties, synthesis, modifications and applications. Journal of Materials Chemistry 20 (2010): 5993-6008.

[14] Bavykin, D. V. and Walsh, F. C. Elongated Titanate Nanostructures and Their Applications. Eur. J. Inorg. Chem. (2009): 977-997.

[15] Kasuga, T., Hiramatsu, M., Hoson, A., Sekino, T., and Niihara, K. Formation of titanium oxide nanotube. Langmuir 14 (1998): 3160-3163.

[16] Mozia, S. et al. Physico-chemical properties and possible photocatalytic applications of titanate nanotubes synthesized via hydrothermal method. Journal of Physics and Chemistry of Solids 71 (2010): 263-272.

[17] Wang, Y. Q., Hu, G. Q., Duan, X. F., Sun, H. L. and Xue, Q. K. Microstructure and formation mechanism of titanium dioxide nanotubes. Chemical Physics Letters 365 (2002): 427-431.

[18] Sreekantan, S. and Wei, L. C. Study on the formation and photocatalytic activity of titanate nanotubes synthesized via hydrothermal method. Journal of Alloys and Compounds 490 (2010): 436-442.

[19] Nakahira, A., Tamai, M., Isshiki, T., and Nishio, K. Synthesis of nanotube from a layered $H_2Ti_4O_9 \cdot H_2O$ in a hydrothermal treatment using various titania sources. Journal of Materials Science 39 (2004): 4239-4245.

[20] Morgan, D. L., Blackford, M. G., Raftery, N. A., Frost, R. L, and Waclawik, E. R. Alkaline hydrothermal kinetics in titanate nanostructure formation. Journal of Materials Science 46 (2011): 548-557.

[21] Kim, Y. S., Kim, G. S., Seo, H. K., and Shin, H. S. Hydrothermal synthesis of titanate nanotubes followed by electrodeposition process. Korean Journal of Chemical Engineering 23 (2006): 1037-1045.

[22] Mao, Y. and Wong, S. S. Size-and Shape-Dependent Transformation of Nanosized Titanate into Analogous Anatase Titania Nanostructures. Journal of the American Chemical Society 128 (2006): 8217-8226.

[23] Bavykin, D. V., Parmon, V. N., Lapkina, A. A., and Walsh, F. C. The effect of hydrothermal conditions on the mesoporous structure of TiO_2 nanotubes. Journal of Materials Chemistry 14 (2004): 3370-3377.

[24] Murakami, N., Kamai, T., Tsubota, T., and Ohno, T. Control of the crystal structure of titanium (IV) oxide by hydrothermal treatment of a titanate nanotube under acidic conditions. CrystEngCom 12 (2010): 532-537.

[25] Bavykin, D. V., Friedrich, J. M., Lapkin, A. A., and Walsh, F. C. Stability of aqueous suspensions of titanate nanotubes. Chemistry of Materials 18 (2006): 1124-1129.

[26] Riss, A., Elser, M. J., Bernardi, J., and Diwald, O. Stability and photoelectronic properties of layered titanate nanostructures. Journal of the American Chemical Society 131 (2009): 6198-6206.

[27] Domínguez, S. D., Murcia, Á. B., Amorós, D. C., and Solano, Á. L. Semihydrogenation of phenylacetylene catalyzed by metallic nanoparticles containing noble metals. Journal of catalysis 243 (2006): 74-81.

[28] Domínguez, S. D., Murcia, Á. B., K. Pradhan, Solano, Á. L. and Amorós, D. C. Semihydrogenation of phenylacetylene catalyzed by palladium nanoparticles supported on carbon materials. Journal of Physical Chemistry C 112 (2008): 3827-3834.

[29] Domínguez, S. D., Murcia, Á. B., Solano, Á. L. and Amorós, D. C. Inorganic materials as supports for palladium nanoparticles: Application in the semi-hydrogenation of phenylacetylene. Journal of Catalysis 257 (2008): 87-95

[30] Sikhwivhilu, L. M., Coville, N. J., Pulimaddi, B. M., Venkatreddy, J., Vishwanathan, V. Selective hydrogenation of o-chloronitrobenzene over palladium supported nanotubular titanium dioxide derived catalysts. Catalysis Communications 8 (2007): 1999-2006.

[31] Sikhwivhilu, L. M. et al. Nanotubular titanate supported palladium catalysts: The influence of structure and morphology on phenol hydrogenation activity. Applied Catalysis A 324 (2007): 52-61.

[32] Murciano, L. T., Lapkin, A. A., Bavykin, D. V., Walsh, F. C., Wilson, K. Highly selective Pd/titanate nanotube catalysts for the double-bond migration reaction. Journal of Catalysis 245 (2007): 272-278.

[33] Panpranot, J., Pattamakomsan, K., James G. Goodwin Jr., Praserthdam, P. A comparative study of Pd/SiO_2 and Pd/MCM-41 catalysts in liquid-phase hydrogenation. Catalysis Communications 5 (2004): 583-590.

[34] Lederhos, C. R., L' Argentiere, P. C., and Fígoli, N. S. 1-Heptyne Selective Hydrogenation over Pd Supported Catalysts. Industrial & Engineering Chemistry Reseach 44 (2005): 1752-1756.

[35] Weerachawanasak, P. et al. Effect of strong metal-support interaction on the catalytic performance of Pd/TiO_2 in the liquid-phase semihydrogenation of phenylacetylene. Journal of Catalysis 262 (2009): 199-205.

[36] Panpranot, J. et al. A comparative study of liquid-phase hydrogenation on Pd/SiO_2 inorganic solvents and under pressurized carbon dioxide: Activity change and metal leaching/sintering. Journal of Molecular Catalysis A: Chemical 253 (2006): 20-24.

[37] Yuan, Z. Y., Su, B. L. Titanium oxide nanotubes, nanofibers and nanowires. Colloids Surf. A 241 (2004): 173-183.

[38] Armstrong, A. R., Armstrong, G., Canales, J., and Bruce, P. G. TiO_2-B nanowires as negative electrodes for rechargeable lithium batteries. Journal of Power Sources 146 (2005): 501-506.

[39] Zhang, M. et al. Effect of annealing temperature on morphology, structure and photocatalytic behavior of nanotubed $H_2Ti_2O_4(OH)_2$. Journal of Molecular Catalysis A: Chemical 217 (2004): 203-210.

[40] Tsai, C. C., and Teng, H. Regulation of the Physical Characteristics of Titania Nanotube Aggregates Synthesized from Hydrothermal Treatment. Chemistry of Materials 16 (2004): 4352-4358.

[41] Panpranot, J., Kontapakdee, K., and Praserthdam , P. Effect of TiO_2 Crystalline Phase Composition on the Physicochemical and Catalytic Properties of Pd/TiO_2 in Selective Acetylene Hydrogenation. Journal of Physical Chemistry B 110 (2006): 8019-8024.

[42] Jongsomjit, B., Wongsalee, T., and Praserthdam, P. Characteristics and catalytic properties of Co/TiO_2 for various rutile: anatase ratios. Catalysis Communications 6 (2005): 705-710.

[43] Yu, H., Yu, J., and Cheng, B. Photocatalytic activity of the calcined H-titanate nanowires for photocatalytic oxidation of acetone in air. Chemosphere 66 (2007): 2050-2057.

[44] Xiao, N., Li, Z., Liu, J., and Gao, Y. Effects of calcination temperature on the morphology, structure and photocatalytic activity of titanate nanotube thin films. Thin Solid Films 519 (2010): 541-548.

[45] Zhu, H. Y. Phase Transition between Nanostructures of Titanate and Titanium Dioxides via Simple Wet-Chemical Reactions. Journal of the American Chemical Society 127 (2005): 6730-6736.

[46] Xu, Y., Fang, X., Xiong, J., and Zhang, Z. Hydrothermal transformation of titanate nanotubes into single-crystalline TiO_2 nanomaterials with controlled phase composition and morphology. Materials Research Bulletin 45 (2010): 799-804.

[47] Hu, F., Ding, F., Song, S., and Shen, P. K. Pd electrocatalyst supported on carbonized TiO_2 nanotube for ethanol oxidation. Journal of Power Sources 163 (2006): 415-419.

[48] Mahata, N. and Vishwanathan,V. Influence of Palladium Precursors on Structural Properties and Phenol Hydrogenation Characteristics of Supported Palladium Catalysts. Journal of Catalysis 196 (2000): 262-270.

[49] Wang, M., Guo, D. and Li, H.. High activity of novel Pd/TiO_2 nanotube catalysts form ethanol electro-oxidation. Journal of Solid State Chemistry 178 (2005): 1996-2000.

[50] Dong, B. et al. High dispersion and electrocatalytic activity of Pd/titanium dioxide nanotubes catalysts for hydrazine oxidation. Journal of Power Sources 175 (2008): 266-271.

APPENDICES

APPENDIX A

CALCULATION FOR CATALYST PREPARATION

The calculation shown below is for 1 wt% Pd on titania and titanate support. The support weight used for all preparation is 1 g.

A.1 Calculation of palladium colloid nanoparticles supported on titania and titanate

Based on 100 g of catalyst used, the composition of the catalyst will be as follows:

Palladium	=	1 g
Support	=	100-1 = 99 g
For 1 g of support		
Palladium required	=	$(1 \times 1)/99 = 0.0101$ g
Molecular weight of Pd	=	106.42 g/mol
Molecular weight of Pd (II) acetate	=	224.42 g/mol

Then, Pd (II) acetate was taken $= \dfrac{M.W.of\ Pd(II)\ acetate \times weight\ of\ Pd\ required}{M.W.of\ Pd}$

$$= \frac{224.42\ g/mol \times 0.0101\ g}{106.42\ g/mol}$$

$$= 0.0213 \text{ g}$$

Palladium colloid nanoparticles were prepared by using Pd (II) acetate 0.2245 g and dispersed in 60 ml of methanol. So the Pd concentration in the resulting Pd nanoparticles/methanol dispersion (mg of Pd/ml of solution) was known.

Then, the mixed solution of methanol was taken

$$= \frac{60\ ml \times 0.0213\ g}{0.2245\ g} = 5.69 \text{ ml}$$

A.2 Calculation of catalyst prepared by wet impregnation

Preparation of catalysts by wet impregnation method is shown as follows:

Based on 100 g of catalyst used, the composition of the catalyst will be as follows:

Palladium = 1 g

Support = 100-1 = 99 g

For 1 g of support

Palladium required = $(1 \times 1)/99 = 0.0101$ g

Molecular weight of Pd = 106.42 g/mol

Molecular weight of Pd chloride = 177.33 g/mol

Then, Pd chloride was taken $= \frac{M.W.of\ Pd\ chloride \times weight\ of\ Pd\ required}{M.W.of\ Pd}$

$= \frac{177.33\ g/mol \times 0.0101\ g}{106.42\ g/mol}$

$= 0.0168$ g

APPENDIX B

CALCULATION FOR CO-CHEMISORPTION

Calculation of the metal active sites, metal dispersion, active metal surface area, and average crystallite size of the catalyst measured by CO-chemisorption is as follows:

Volume of active gas dosed from a loop (V_{inj})

$$V_{inj} = V_{loop} \times \frac{T_{std}}{T_{amb}} \times \frac{P_{amb}}{P_{std}} \times \frac{\%A}{100\%}$$

Example: Volume Dosed Using 100 % Active Gas

V_{loop}	=	loop volume injected	86 μL
T_{amb}	=	ambient temperature	298 K
T_{std}	=	standard temperature	273 K
P_{amb}	=	ambient pressure	743 mmHg
P_{std}	=	standard pressure	760 mmHg
%A	=	% active gas	100 %

$$V_{inj} = 86\ \mu L \times \frac{273\,K}{298\,K} \times \frac{743\ mmHg}{760\ mmHg} \times \frac{100\,\%}{100\,\%}$$

Volume chemisorbed (V_{ads})

$$V_{ads} = \frac{V_{inj}}{m} \times (\frac{B - A}{B})$$

Example: CO Chemisorption on Pd/TNT

V_{inj}	= volume injected	0.07780 cm^3
m	= mass of sample	0.0400 g
A	= area of CO peak after adsorption	0.01335
B	= average area of the last peak	0.01617

Peak	Area
1	0.01335
2	0.01623
3	0.01614
4	0.01616
5	0.01617

$$V_{ads} = \frac{0.07780}{0.0400\,g} \times (\frac{0.01617 - 0.01335}{0.01617}) = 0.3397 \text{ cm}^3/\text{g}$$

% Metal dispersion

$$\%D = S_f \times \frac{V_{ads}}{V_g} \times \frac{M.W.}{\%M} \times 100\% \times 100\%$$

Example: % Dispersion of Pd/TNT catalyst

S_f	=	stoichiometer facter, CO on Pd	1
V_{ads}	=	volume adsorbed	0.3397 cm^3/g
V_g	=	molar volume of gas at STP	22414 cm^3/mol
m.w.	=	molecular weight of the metal	106.42 g/mol
% M	=	weight percent of the active metal (from ICP)	0.51 %

$$\%D = 1 \times \frac{0.3397\,cm^3/g}{22414\,cm^3/mol} \times \frac{106.42\,g/mol}{0.51\%} \times 100\% \times 100\% = 31.7\ \%$$

Pd active sites

$$Pd\ active\ sites = S_f \times \frac{V_{ads}}{V_g} \times N_A$$

S_f	=	stoichiometry factor, CO on Pd	1
V_{ads}	=	volume adsorbed	0.5976 cm^3/g
V_g	=	molar volume of gas at STP	22414 cm^3/mol
N_A	=	Avogadro's number	6.023×10^{23} molecules/mol

$$Pd\ active\ sites = 1 \times \frac{0.3397\,cm^3/g}{22414\,cm^3/mol} \times 6.023\times10^{23}\ molecules/mol$$

$$= 9.13 \times 10^{18}\ \text{molecules/g}$$

Active metal surface area (per gram of metal)

$$MSA_s = S_f \times \frac{V_{ads}}{V_g} \times \frac{100\%}{\%M} \times N_A \times \sigma_m \times \frac{m^2}{10^{18}\,nm^2}$$

S_f	=	stoichiometry factor, CO on Pd	1
V_{ads}	=	volume adsorbed	0.3397 cm^3/g
V_g	=	molar volume of gas at STP	22414 cm^3/mol
% M	=	weight percent of the active metal	0.8 %
N_A	=	Avogadro's number	6.023×10^{23} molecules/mol
σ_m	=	cross-sectional area of active metal atom	0.0787 nm^2

$$MSA_s = 1 \times \frac{0.3397\,cm^3/g}{22414\,cm^3/mol} \times \frac{100\%}{0.51\%} \times 6.02\times10^{23}\ \frac{molecules}{mol} \times 0.0787\,nm^2 \times \frac{m^2}{10^{18}\,nm^2}$$

$$= 141.23\ m^2/g_{metal}$$

Average crystallite size

$$d = \frac{F_g}{\rho \times MSA_s} \times \frac{m^3}{10^6\,cm^3} \times \frac{10^9\,nm}{m}$$

F_g	=	crystallite geometry factor (hemisphere = 6)	6
ρ	=	specific gravity of the active metal	12.0 g/cm^3
MSA_s	=	active metal surface area per gram of metal	173.39 m^2/g_{metal}

$$d = \frac{6}{12.0\,g/cm^3 \times 141.23\,m^2/g} \times \frac{m^3}{10^6\,cm^3} \times \frac{10^9\,nm}{m}$$

$$= 3.5\ \text{nm}$$

APPENDIX C

CHROMATOGRAMS FROM GAS CHROMATOGRAPHY

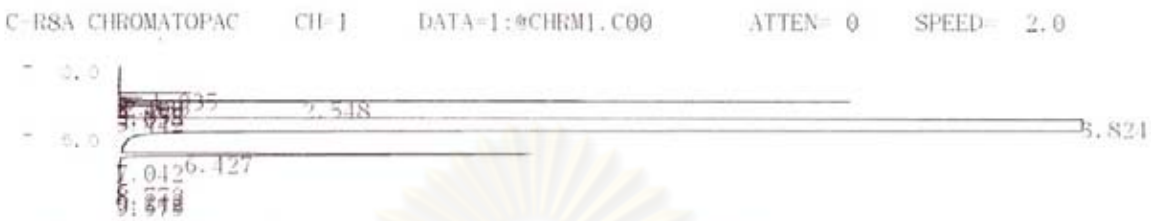

** CALCULATION REPORT **

CH	PKNO	TIME	AREA	HEIGHT	MK	TDNO	CONC	NAME
1	1	1.935	107	76			0.0274	
	2	2.336	41	24			0.0106	
	4	2.548	1430	761			0.3652	
	5	2.852	109	46	V		0.0277	
	6	3.058	44	12	V		0.0113	
	7	3.442	49	4	V		0.0126	
	8	3.824	386607	15609	SV		98.6933	
	9	6.427	3256	411	T		0.8311	
	11	8.772	82	9			0.0209	
		TOTAL	391726	16952			100	

Figure C.1 Chromatograms from gas chromatography

Table C.1 Data from gas chromatography

Peak number	Time (min)	Name
1	1.935	Heptane
2	2.548	Heptene
3	3.824	Toluene (solvent)
4	6.427	1-Heptyne

APPENDIX D

CALIBRATION CURVE OF 1-HEPTYNE AND 1-HEPTENE

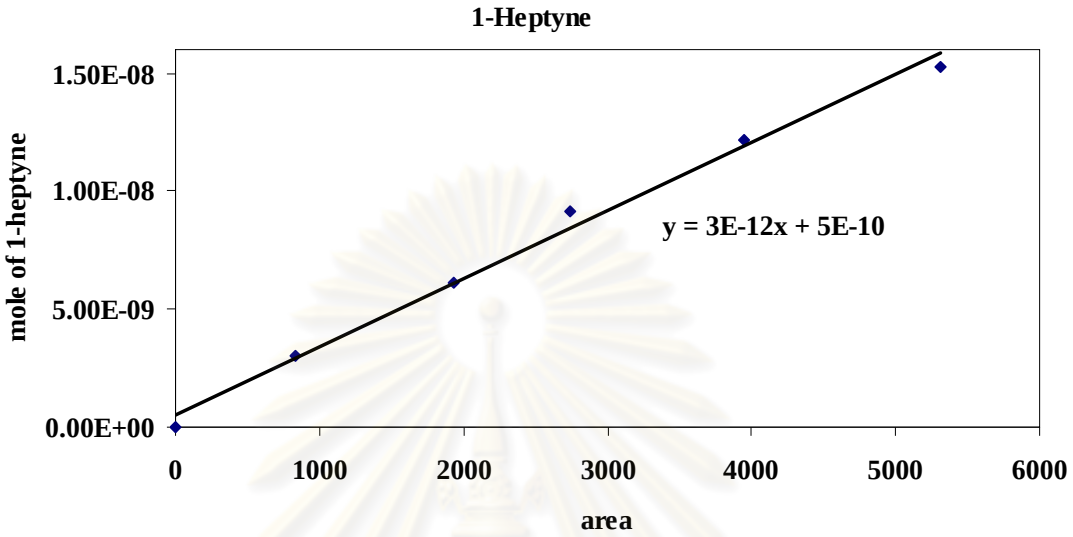

Figure D.1 Calibration curve of 1-heptyne

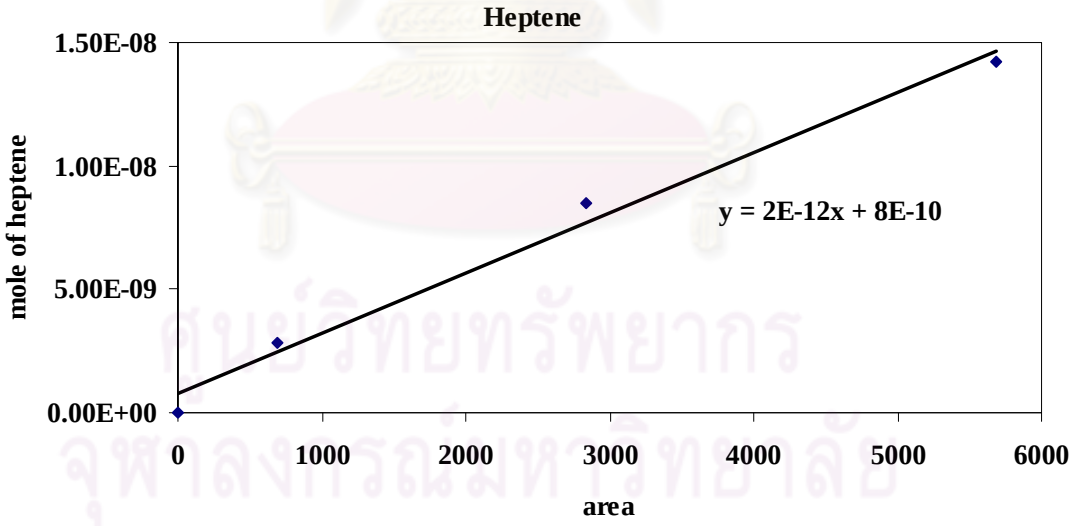

Figure D.2 Calibration curve of 1-heptene

APPENDIX E

CONVERSION, SELECTIVITY, AND YIELD AT VARIOUS REACTION TIMES

The conversion, selectivity, and yield of 1-heptyne hydrogenation for all catalysts are shown the table.

Table E.1 Conversion of 1-heptyne

Catalysts	Conversion (%)			
	5 min	10 min	30 min	40 min
Pd/TiO_2 com	21	50	94	100
Pd/TNT	40	86	100	100
Pd/TNW	32	61	100	100
Pd/TNT_600	40	60	100	100
Pd/TNT_soni	55	91	100	100
Imp_stir	23	39	86	100
Imp_soni	25	45	98	100

Table E.2 Selectivity of 1-heptene

Catalysts	Selectivity (%)			
	5 min	10 min	30 min	40 min
Pd/TiO_2 com	92	94	93	48
Pd/TNT	92	94	63	62
Pd/TNW	93	95	66	65
Pd/TNT_600	93	95	68	62
Pd/TNT_soni	92	74	70	62
Imp_stir	96	97	95	66
Imp_soni	96	94	94	82

Table E.3 Yield of 1-heptene

Catalysts	Yield (%)			
	5 min	**10 min**	**30 min**	**40 min**
Pd/TiO_2 com	19.32	47.00	87.42	48.00
Pd/TNT	36.80	80.84	63.00	62.00
Pd/TNW	29.76	57.95	66.00	65.00
Pd/TNT_600	37.20	57.00	68.00	62.00
Pd/TNT_soni	50.60	85.54	70.00	62.00
Imp_stir	22.08	37.83	81.70	66.00
Imp_soni	24.00	43.20	92.12	82.00

APPENDIX F

CALCULATION OF 1-HEPTYNE CONVERSION AND 1-HEPTENE SELECTIVITY

The catalytic performance for the 1-heptyne hydrogenation was evaluated in terms of activity for 1-heptyne conversion and 1-heptene selectivity.

Activity of the catalyst performed in term of 1-heptyne conversion. The conversion is defined as moles of 1-heptyne converted with respect to 1-heptyne in feed:

1- heptyne conversion (%)

$$= \frac{(mole\ of\ 1-heptyne\ in\ feed)-(mole\ of\ 1-heptyne\ in\ product)}{mole\ of\ 1-heptyne\ in\ feed}\times 100$$

Selectivity of product is defined as mole of 1-heptene formed with respect to mole of 1-heptene and heptane was obtained:

$$\text{Selectivity of 1-heptene} = \left(\frac{mole\ of\ 1-heptene\ \ formed}{mole\ of\ total\ products}\right)\times 100$$

APPENDIX G

CALCULATION OF TURNOVER OF FREQUENCY

$$\text{TOF} = \frac{rate}{number\ of\ active\ site}$$

$$= \frac{molecules\ substrate\ converted}{g\ cat \times \min} \times \frac{g\ cat}{active\ site} \times \frac{\min}{s}$$

While, metal active site = molecule/ g catalysts

Then,

TOF = $[s^{-1}]$

VITA

Mr. Somjit Putdee was born in September 17 th, 1986 in Mahasarakham, Thailand. He finished high school from Nakhawittayakom School, Mahasarakham in 2004. After that, he studied at Silpakorn University, Nakornpathom, Thailand for 4 years and received Bachelor's Degree from the department of Chemical Engineering in March 2009. Then, he required to study in the Master's Degree at the department of chemical engineering, Chulalongkorn University in 2009.

List of publication

In November 2010, he participated in the 17th Regional Symposium on Chemical Engineering (RSCE 2010), Bangkok, Thailand for oral presentation and published for "Influence of preparation conditions on the formation of titanate nanotubes by hydrothermal method".